DOI:10.14753/SE.2023.2805

Application of cyclodextrins for capillary electrophoretic analysis of gangliosides and manipulation of their membrane content

PhD thesis

Orsolya Geda

Doctoral School of Pharmaceutical Sciences

Semmelweis University

Supervisor: Éva Szökő, DSc

Official reviewers: Levente Szőcs, PhD
Ida Fejős, PhD

Head of the Complex Examination Committee:

István Antal, PhD

Members of the Complex Examination Committee:

Krisztina Németh, PhD
László Kőhidai, CSc

Budapest
2022

DOI:10.14753/SE.2023.2805

Table of contents

DOI:10.14753/SE.2023.2805

DOI:10.14753/SE.2023.2805

DOI:10.14753/SE.2023.2805

List of Abbreviations

4-AP	4-aminopyridine
ACD	alpha-cyclodextrin
AD	Alzheimer's disease
BCD	beta-cyclodextrin
CD	cyclodextrin
CE	capillary electrophoresis
CE-LIF	capillary electrophoresis-laser induced fluorescence
CE-MS	capillary electrophoresis–mass spectrometry
Cer	ceramide
DIMEB	heptakis(2,6-di-O-methyl)-beta-cyclodextrin
DL-TBOA	DL-threo-β-benzyloxyaspartic acid
DMSO	dimethyl sulfoxide
DS	degree of substitution
EOF	electroosmotic flow
ESI	electrospray ionization
FBS	fetal bovine serum
Gal	galactose
GalNAc	N-acetylgalactosamine
GCD	gamma cyclodextrin
GCS	gylcosylceramide synthase
Glc	galactose
GSL	glycosphingolipid
HEPES	4-(2-hydroxyethyl)-1-piperazine ethanesulfonic acid
HILIC	hydrophilic interaction liquid chromatography
HPACD	(2-hydroxypropyl)-alpha-cyclodextrin
HPBCD	(2-hydroxypropyl)-beta-cyclodextrin
HPLC	high pressure liquid chromatography
IC_{50}	half maximal inhibitory concentration
ICH	International Conference on Harmonization
IS	internal standard
LBSA	lipid-bound sialic acid

LC-MS	liquid chromatography coupled to mass spectrometry
LDH	lactate dehydrogenase
LLE	liquid-liquid extraction
LOD	limit of detection
LOQ	limit of quantification
LTP	long-term potentiation
MAG	myelin-associated glycoprotein
MBCD	methyl beta-cyclodextrin
MEKC	micellar electrokinetic chromatography
MS	mass spectrometry
MTT	3-(4,5-dimethylthiazol-2-yl)-2,5-diphenyltetrazolium bromide
NaOH	sodium hydroxyde
NBD-F	4-fluoro-7-nitrobenzofurazan
NeuAc	N-acetyl-neuraminic acid
NPC	Niemann-Pick disease, type C
PBS	phosphate buffered saline
PKC	protein kinase C
PLCγ	phosphoinositide phospholipase C gamma
QC	quality control
QTOF/MS	quadrupole time of flight mass spectrometer
RAMEA	randomly methylated alpha-cyclodextrin
RAMEB	randomly methylated beta-cyclodextrin
RSD	relative standard deviation
SBEBCD	sulfobutyl ether-beta-cyclodextrin
SDS	sodium dodecyl sulfate
SEM	standard error of mean
TLC	thin-layer chromatography
TrkA	tropomyosin receptor kinase A

DOI:10.14753/SE.2023.2805

1. Introduction

1.1. Biological functions of gangliosides

Gangliosides are sialic acid-containing glycosphingolipids (GSLs) of the plasma membrane and are highly abundant in the nervous system of vertebrates (1), where they are considered to play a vital role in normal cell functions. Gangliosides are ubiquitously found in most tissues but are particularly enriched on neuronal cells, where they contribute significantly to the cell surface glycans (2). They are considered to be localized in membrane microdomains, also known as lipid rafts (3), where their functions include interactions with membrane proteins located in the same membrane and regulation of cell-cell recognition with ganglioside binding proteins on opposing cells (4, 5). Both the hydrophilic and hydrophobic parts of gangliosides can have a wide variety of structures, which raises the possibility of the functional significance of the structural diversity of both parts. Although considerable progress has been made towards a better understanding of the function of gangliosides, our knowledge of their mechanism of action is still largely incomplete.

1.1.1. Structure and nomenclature of gangliosides

Gangliosides are composed of an oligosaccharide chain linked to a highly hydrophobic ceramide (Figure 1). Heterogeneity in the composition of the glycan group is high and nearly 200 ganglioside glycoforms are identified so far, furthermore, the structural complexity increases with heterogeneity in the ceramide lipid moieties (6), but only a few gangliosides are abundant in neural tissues. Ceramide include a long-chain amino alcohol called sphingosine connected to a fatty acid by an amide linkage. In the nervous system of mammals, sphingosine typically is of 18 or 20 carbons (7) and stearic acid is the major fatty acid component (>80%) of gangliosides (1). The oligosaccharide portion contains one or more N-acetylneuraminic acid, which is the predominant sialic acid in humans (2). Sialic acids have a pK_A value of 2.6 making the molecule negatively charged at physiological pH (8). The oligosaccharide portion is based on a chain constituted by neutral sugars of different numbers, linked to each other in a specific order.

DOI:10.14753/SE.2023.2805

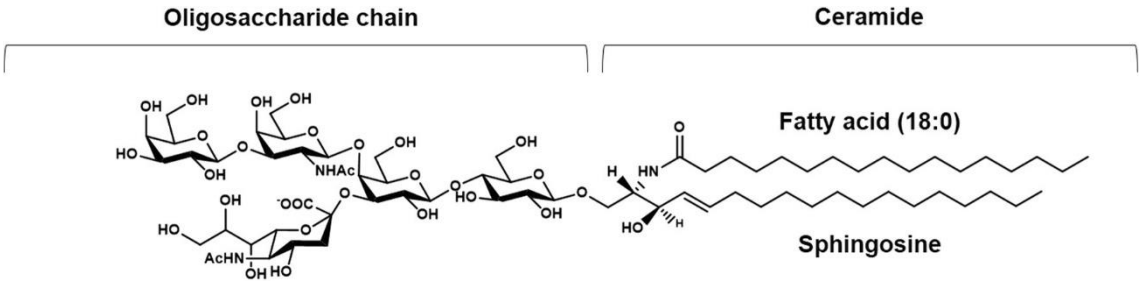

Figure 1. Structure of GM1, one of the most abundant gangliosides in the adult brain (9). Copyright © 2021 Chiricozzi et al, CC BY 4.0.

The nomenclature of GSLs, including gangliosides is based on their glycan part. According to the nomenclature of Svennerholm, the core structure of neutral sugars (full or truncated) defines the name of a respective series, in which the "ganglio-series" contain glucose, galactose and N-acetylgalactosamine, attached in a defined order to ceramide. The capital letter "G" stands for ganglioside, followed by a capital letter designating the total number of sialic acids ("A" = 0, "M" =1, "D" = 2, "T" = 3, "Q" = 4, "P" = 5, "H" = 6, "S" = 7), an Arabic number based on the length of the neutral sugar core. Initially, it was assumed that this could not exceed five, so the number "1" refers to (5 – "1" = 4), thus 4 neutral sugars. This could be followed by a lowercase letter standing for the number of sialic acid residues on the 3-hydroxyl of the innermost galactose ("a" = 1, "b" = 2, "c" = 3). However, in the case of monosialogangliosides lower case letter is optional and most often omitted (8, 10, 11).

In mammals, the sialic acid residues are typically attached to the galactosyl unit by an α-2,3-linkage and by an α-2,8-linkage to other sialic acids (8). The most abundant ganglioside outside the nervous system is the "simple" GM3, which is the first ganglioside in the biosynthetic pathway with a core structure of lactosylceramide linked to one sialic acid (Figure 2). The most abundant gangliosides in the nervous system have more complex sugar structure, characterized by the Galβ1-3 GalNAcβ1-4 Galβ1-4 GlcβCer core (11, 12).

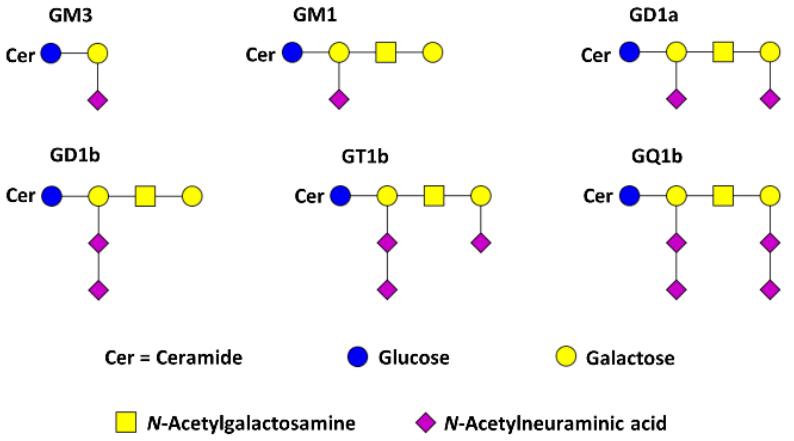

Figure 2. Structures of major neuronal (GM1, GD1a, GD1b, GT1b, GQ1b) and extraneural (GM3) gangliosides (13). Copyright © 2021 Geda et al, CC BY-NC-ND 4.0.

1.1.2. Gangliosides as parts of membrane microdomains

The structure of gangliosides results in a highly amphiphilic molecule, enabling both hydrophilic and hydrophobic interactions. Gangliosides are inserted mainly into the external leaflet of plasma membrane with their hydrophobic ceramide tail, while their variable oligosaccharide chain facing towards the extracellular space (8). They are reported to be enriched in specific microdomains of the plasma membrane, tightly packed together with sphingomyelin and cholesterol (3). These membrane microdomains, or so-called lipid rafts are considered to create a relatively ordered phase compared to the surrounding membrane, which acts as a platform for membrane proteins. The composition of these microdomains is believed to influence the organization of various molecules involved in cell signaling (3). Both their carbohydrate chain and the lipid tail have specific physicochemical features that favor the formation of microdomains. For example, the geometry of the oligosaccharide headgroup, the carbohydrate-water interactions, their long, saturated alkyl chains as well as their capability of forming hydrogen-bond network at the lipid-water interface are all specific properties that strongly suggest a role in the formation of liquid-ordered microdomains in the membrane (3).

Cholesterol, thought to be the main component of lipid rafts, is known to modulate membrane fluidity and interacts preferentially with long, saturated alkyl chains such as those found in gangliosides, which interaction also supports the formation of liquid-

ordered microdomains (14, 15). Although, it should be noted, that the lipid raft hypothesis is widely accepted, there is also skepticism about whether rafts exist due to the technical challenges of studying them in living cells (16, 17).

It was observed, that gangliosides undergo phase separation without the presence of cholesterol (18) for which the main driving force is thought to be their hydrophilic headgroup that is remarkably different than that of phospholipids (12). The clustering allows the minimization of the interfacial free energy and according to the observations, the volume of the oligosaccharide head group determines the level of phase separation and also the geometrical changes in the membrane. The larger the headgroup, the segregation is more pronounced and the curvature of the resulting ganglioside-rich cluster is more positive (12). The volume of the sugar head group is also influenced by the presence of hydrating water associated with the oligosaccharide chain, which is remarkably high (22 to 60 water molecules compared to 6-7 in case of a phosphocholine headgroup (19)) proposed that the presence of hydrating water is likely relevant in avoiding the electrostatic repulsion generated by the negative charges on the sugar chain, and moreover, a network of hydrogen bridges could considerably contribute to the stabilization of the ganglioside clusters.

1.1.3. Gangliosides in the nervous system

The concentration and structure of gangliosides undergo major changes during brain development (20), due to the spatiotemporal expression, posttranslational modification and subcellular localization of glycosyltransferases (21). At early stages of development, gangliosides with simple carbohydrate chain are present, while later complex gangliosides are more predominant (2). Their essential role in brain development has been shown by systematic deletion of gylcosylceramide synthase (GCS) gene in mice that caused early embryonic death (22), while targeted deletion of GCS gene in neurons resulted in dysfunction of cerebellum and peripheral nerves as well as changes in neuronal morphology and myelin sheaths and death three weeks after birth (23). In the adult brain of humans as well as other mammals, the most abundant gangliosides are GM1, GD1a, GD1b, GT1b and GQ1b, where their concentration is approximately 10-fold higher than that in the peripheral tissues (24-26) (Figure 2). However, some of these gangliosides

occur also in peripheral tissues, such as GM1 in the liver (25, 27), muscle (28) and adipose tissue (29).

The pattern and level of neuronal gangliosides also change during aging: from age of 70 years, a rapid decline was shown in ganglioside concentration (30). The distribution of gangliosides also shows large differences between brain areas (31).

The level and structure of the ceramide moieties of gangliosides also show developmental changes: the ratio of C18 and C20 sphingosine is related to different developmental stage of the brain. During fetal life, C20 sphingosine is not present, but increases slowly with neurodevelopment and aging, becoming predominant in addition to C18 sphingosine (7). It was hypothesized that the heterogeneity of lipid part of gangliosides may have a modulating effect on the fluidity and organization of membrane microdomains, which may influence lipid-protein interactions (7).

Most research, however, has focused on the functions of the different ganglioside glycoforms, since the carbohydrate head group can interact with proteins located laterally in the membrane or with proteins from other cells. Studies have shown that gangliosides interact with an exceptionally large number of membrane proteins, and affect essential functions of nerve cells, such as axon-myelin stability, neurite outgrowth, neurotransmitter release and calcium signaling.

Two of the most abundant gangliosides in the brain, GD1a and GT1b, have been shown to play a crucial role in myelin stability and proper axonal function by being ligands for myelin-associated glycoprotein (MAG, Siglec-4), a sialic acid-binding lectin expressed in the membranes of myelinating oligodendrocytes in the central nervous system and Schwann cells in the peripheral nervous system. In the absence of GD1a and GT1b, increased number of degenerated axons, loosened myelin sheaths in different areas of the spinal cord (32) and demyelination in the peripheral nerves were also observed (33). Apparently, MAG preferentially binds to NeuAcα2-3 Galβ1-3 GalNAc terminal sequence shared by GD1a and GT1b (34).

Several studies have shown that exogenous addition of gangliosides to the cells can induce neurite outgrowth and axonal sprouting in regenerating axons *in vitro* (35, 36). Moreover, it was revealed that the focal generation of GM1 is necessary for the establishment of neuronal polarity *via* the enhancement of TrkA activity (37). Recently it was suggested that the observed neurotrophic effect of gangliosides might be a result of a direct interaction between GM1 and TrkA receptor and a subsequent activation of PLCγ and PKC pathway, leading to the increase of cytosolic Ca^{2+} necessary for cell differentiation (38).

It was shown that gangliosides affect other receptor tyrosine kinases such as insulin receptor (IR) (39). Increased level of GM3 was reported to inhibit IR by an interaction with a lysine residue of the protein (40). This interaction disrupts the binding of IR to caveolin, a crucial protein in insulin signaling, that can result in insulin resistance (29, 41-43). These observations are of peripheral tissues, and it is not yet known whether this phenomenon is also present in the brain. Interestingly, both increase in GM3 level and decrease in brain IR signaling was observed in Alzheimer's disease (44, 45), however the causal role has not been investigated.

The role of lipid rafts and gangliosides was also examined in synaptic transmission. Several neurotransmitter receptors (NMDA, AMPA, $GABA_A$ receptors) and transporters (serotonin, norepinephrine, glutamate transporter) were shown to localize in membrane microdomains (46). Specifically, the role of gangliosides in neurotransmitter signaling was studied and their contribution to neurotransmitter release and ion-transport was revealed (47-51). Voltage-dependent calcium channels (52, 53), as well as plasma membrane Ca^{2+}-ATPase (54) was shown to be influenced by gangliosides. The proposed explanation on the modulating effect of gangliosides on calcium channel activity is that they alter membrane fluidity and/or that Ca^{2+} binds to negatively charged sialic acid residues at the synaptic membrane, resulting in high Ca^{2+} concentration in areas adjacent to calcium channels, which facilitates the ion-transport (49). Electrophysiological studies revealed that the addition of tetrasialoganglioside GQ1b induces long-term potentiation (LTP) and enhances ATP-induced LTP in guinea pig hippocampal slices of CA1 neurons (55).

Both the absence and excess of gangliosides could lead to severe neurodegenerative conditions, which emphasizes their crucial role in normal neuronal functions. Besides, several diseases are known to be associated with altered ganglioside metabolism that results in some form of neurodegeneration (2). In GM1 gangliosidoses, and GM2 gangliosidoses including Tay-Sachs and Sandhoff diseases, the inherited deficiency of catabolic enzymes leads to accumulation of gangliosides in lysosomes, resulting in delay in development and early onset neurodegeneration (56, 57). In addition, growing evidence suggests that alterations in ganglioside levels and profile occur in Alzheimer's disease, Huntington's disease and Parkinson's disease (58).

1.2. Techniques for separation of gangliosides

Several analytical techniques have been developed for the analysis of gangliosides. Most commonly, they are isolated by a liquid-liquid extraction (LLE) method (59), followed by analysis using the method of choice. One of the earliest approaches to quantify total ganglioside level is the determination of the lipid-bound sialic acid (LBSA) content of the sample by spectrophotometric method (60). Then, a separation technique is required to estimate the levels of individual ganglioside species. They can be analyzed in their native form and in some methods, derivatization is performed in order to decrease their detection limit, since they have a maximum absorption at 197 nm (61), where several other compounds have strong absorption. Given their complex structure, the aim may be to analyze them according to their lipid or carbohydrate portion (62, 63). This section provides a brief overview of separation techniques developed for ganglioside analysis, including methods of thin-layer chromatography (TLC), high pressure liquid chromatography (HPLC), liquid chromatography coupled to mass spectrometry (LC-MS) and capillary electrophoresis (CE).

1.2.1. TLC methods

TLC with colorimetric detection is the most widely used separation method to date, where the levels of individual gangliosides are expressed as a percentage of the total LBSA content, according to their band intensity. Separation of gangliosides according to their carbohydrate chain can be achieved by TLC methods. Although this method has some advantages, such as low instrumentation and running cost, its limitations are the relatively

poor reproducibility and sensitivity, and the high organic solvent consumption. The sensitivity of TLC techniques can be significantly improved by immunostaining or radioimaging detection (64-67).

1.2.2. HPLC and LC-MS methods

HPLC methods were also developed for the separation of gangliosides, however these were characterized by very long elution time or the need of off-line monitoring of underivatized gangliosides by TLC due to the higher UV absorbance of eluent solvents than that of gangliosides (50, 68). Although some progress was made with the development of HPLC methods with direct UV detection (61, 69, 70), these were replaced by LC-MS methods as the technique has become more widespread.

Among LC-MS methods, the two categories are currently used are hydrophilic interaction liquid chromatography (HILIC) using silica and amino columns, and reversed-phase HPLC, followed by characterization by MS (71). In HILIC methods, gangliosides are separated based on their hydrophilic carbohydrate chain, but almost no separation occurs between the different lipoforms (71). Using reversed-phase columns, the separation is based on the ceramide length, but co-elution of ganglioside glycoforms with the same alkyl chain length is problematic (71).

LC-MS methods were shown to be valuable for the identification of minor components from biological samples, due to their high sensitivity (nM range) (72-74). Adequately validated methods for the quantification of the most abundant gangliosides from biological samples, however, are limited. Methods for the quantitative determination of some selected gangliosides in human plasma (74, 75) or human cerebrospinal fluid (76) have been reported. Methods using external calibration were reported for the determination of rat (77), mouse and bovine gangliosides (71), but this calibration approach is not entirely reliable for analyzing biological samples.

1.2.3. CE methods

Relatively few CE methods, aiming at the separation of gangliosides, has been reported so far. The pioneering CE works focused on the investigation of separation conditions of ganglioside standards. Gangliosides have a strong amphiphilic character and were shown

to form micelles and mixed micelles in aqueous solutions (78, 79). This property was a main limiting factor in their CE separation as monomers and it was reported that surfactants, urea and organic solvents were tested, but none of these improved the separation (80). On the other hand, with the use of alpha-cyclodextrin (ACD) as buffer additive, separation was achieved and it was suggested that native ACD can disrupt the micelles *via* inclusion complex formation with the lipid moiety that enables the separation of standard gangliosides (GM1, GD1a, GD1b, GT1b) (80). Native beta-cyclodextrin (BCD) and gamma-cyclodextrin (GCD) had minimal effect on the separation, although the concentration ranges tested were not reported (80, 81). In subsequent CE works (81, 82) it was also demonstrated that the complexation of borate with the oligosaccharide residue is necessary for the separation of GD1a and GD1b structural isomers, as it may provide additional negative charge on the analytes.

Although CE coupled to mass spectrometry (CE-MS) represents a powerful analytical technique offering fast and high-resolution separation and subsequent mass information and molecular characterization, only a few CE-MS method has been reported to date. An off-line CE-ESI/QTOF/MS method was developed for screening ganglioside mixture from bovine brain, where the identification of ganglioside glycoforms and their main lipoforms was shown (83). In another method, using CE-ESI/MS, sensitivity improvement was reported by reducing ion-suppression with the removal of non-volatile buffer additives borate and ACD (84).

Various derivatization methods have also been developed to increase the sensitivity of CE methods. The method, reported by Mechref and co-workers (82) involved the formation of an amide-bond between carboxylic group of sialic acids and the amino-group of the derivatization agents, *i.e.* sulfanilic acid or 7-aminonaphthalene-1,3-disulfonic acid, providing a chromophore or fluorophore respectively, and a permanent negative charge of the analytes over a wide pH range. However, a method involving the derivatization of sialic acids may be difficult to transfer to biological samples, as the different number of sialic acids on the different ganglioside glycoforms may lead to multiple labeling and formation of by-products resulting a complex electropherogram. In other CE methods, fatty acid-free (lyso) ganglioside standards were acylated with commercially available succinimidyl esters of BODIPY fluorophores (85, 86). The labor-

intensive derivatization procedure enabled the ymol-detection of fluorescently labeled standards by capillary electrophoresis-laser induced fluorescence (CE-LIF) method, where their separation was performed using micellar electrokinetic chromatography (MEKC) with ACD or BCD as additives (85). It has been shown, however, that the reproducibility of the derivatization procedure may be limited in real biological samples, especially when the analyte concentration is low (87).

Among these CE methods, only the separation of underivatized gangliosides was demonstrated in some biological samples (apricot seed, deer antler and rat brain samples), but with poor separation efficiency (80). The separation of four highly abundant neuronal gangliosides was examined, but GQ1b was not investigated. Furthermore, the most abundant extraneural ganglioside, GM3, was neither studied. For these reasons, no validated CE method for the quantification of gangliosides from biological samples has been reported.

1.3. Cyclodextrins and their complexation with lipids

CDs are cyclic oligosaccharides consisting of α-1,4-glucopyranose units. The main types of CDs ACDs, BCDs and GCDs are composed of 6, 7 or 8 glucopyranose units, respectively. Due to their relatively hydrophobic cavity and hydrophilic surface, they are able to form host-guest inclusion complexes with a broad range of hydrophobic molecules (88). Therefore, they are extensively used in drug formulation, to improve water solubility and bioavailability of drugs, in addition to food, cosmetic and environmental applications (89, 90). The number of the glucose units determines the cavity size and. Due to the chair conformation of the units, CDs are cone-shaped molecules with the primary hydroxyl groups extending from the narrower side and the secondary hydroxyl groups extending from the wider side making them hydrophilic (88).

Natural or native CDs are hydrophilic, but their aqueous solubility may be limited, especially in the case of BCD (91). The poor water solubility can be explained by the presence of the hydrogen bonding C2 and C3 OH groups, which in native BCD leads to the formation of the so-called complete secondary belt, resulting in an inflexible structure and a decreased ability of the molecule to form intermolecular hydrogen bond. In ACD, the hydrogen-bond belt is incomplete, because of the distorted position of one

glucopyranose unit, and GCD is a non-coplanar, more flexible structure, therefore, they both possess higher water solubility than BCD (92). Substitution of hydroxyl groups even with hydrophobic groups can lead to dramatic solubility improvements (91, 93). Randomly methylated-beta-cyclodextrin (RAMEB), hydroxypropyl-beta-cyclodextrin (HPBCD) and sulfobutyl ether-beta-cyclodextrin (SBEBCD) are examples of chemically modified BCDs, which are used as drug excipients (94). The physicochemical characteristics of CDs, including water solubility and complexation capability, depend not only on the type of substituent, but their location on the CD molecule and the number of substituents per CD. The degree of substitution (DS) in CD chemistry is defined as the average number of substituents per CD molecule (93).

The cavity of CDs is lined by glycosidic oxygen bridges and hydrogen atoms creating a slightly apolar cavity, which is occupied by water in aqueous solutions. The presence of water in the cavity is energetically unfavoured, and can be substituted by molecules that are less polar than water, which is probably the key driving force for complex formation. Non-covalent interactions such as hydrophobic interactions, van der Waals interactions or electrostatic interactions can occur between the guest molecule and the CD. The host:guest ratio is most frequently 1:1, but 2:1, 1:2, 2:2 and other combinations exist too (92, 95). In aqueous solutions inclusion complexes are in dynamic equilibrium with free guest and CD molecules (92).

Several types of medicinal products contain CDs, such as oral, nasal, ocular products or parenteral solutions. At least six types of CDs are used currently in medicines: ACD, BCD, GCD, HPBCD, SBEBCD and RAMEB. The oral availability of CDs is very low, however, high doses my cause reversible diarrhea and cecal enlargement in animals. Topical application of CDs may influence tissue permeability, depending on the amount. Parenteral administration of relatively low doses of ACD, BCD and RAMEB showed renal toxicity and they are not suitable given intravenously (94).

Considering the hydrophobic or amphiphilic nature of lipids, they can also be entrapped into CDs. Encapsulation of several lipid classes have been investigated, moreover, products utilizing the CD/lipid interaction have been marketed, such as food or cosmetic products (96, 97). CD/lipid interactions are also being investigated because of their

application as drug excipients and potential influence on membrane lipids. As part of their safety profile, cellular interactions of CDs have also been studied. It was found that the hemolytic activity of native CDs is decreased in the order BCD>ACD>GCD and these differences were attributed to the different solubilization rates of membrane components (98). Due to their internal cavity size, BCD and its derivatives are able to form stable complexes with cholesterol (99) and it was shown that BCDs extract cholesterol from the plasma membrane too (100). Comparing CDs with similar substituents but different cavity sizes, their interaction with cholesterol decreases in the order BCD>>GCD>ACD suggesting that cavity size plays the main role in complex formation (99).

The type of substituents also influences the complex forming capability of CDs. Methylated BCDs (MBCDs) have been shown to be the most potent in solubilizing cholesterol (101-103), and they were also the most toxic (104). Therefore, the application of MBCDs is permitted only in nasal and ocular products (94). On the other hand, MBCDs are widely used in biochemical experiments as lipid raft disrupting agents due to their cholesterol extracting capability. The effect of MBCDs on other membrane lipids has been also studied (105), but data on their influence on gangliosides are limited, however they are considered to be lipid raft components as well and have significant regulatory role in several cellular functions.

Utilizing the CD/lipid interaction, HPBCD is under clinical investigation as a drug candidate in Niemann-Pick type C disease (NPC), where it has been reported to alleviate cholesterol accumulation in lysosomes (106). HPBCD have also been used for cholesterol extraction *in vitro*, however, due to its inferior efficiency, it is not as common as MBCDs (107).

In addition to cholesterol, CDs may form complexes with fatty acids, which is also strongly influenced by the cavity size of CDs. Native ACD provides a better fit to complex saturated fatty acids than BCD. However, BCD form complexes with unsaturated fatty acids more readily than with saturated ones. In general, GCD has the lowest affinity to form complexes with fatty acids, because its larger cavity size cannot provide stable interaction for complex formation. As in the case of cholesterol, solubility experiments with fatty acids suggest that methylated CDs are the most potent solubilizing

agents (103). Complexes of different stoichiometry can be formed with fatty acids: there are about 6 CH2 units per a CD molecule, therefore C18 stearic acid can form complex with an average of three CD molecules (99, 103).

Based on their selective lipid recognizing properties, CDs might be valuable tools in *in vitro* studies for modulating the lipid content in order to study their functions.

2. Objectives

Due to the growing evidence for the regulatory functions of gangliosides in many cellular functions and their possible pathological role in various diseases, there is a need for an analytical method to quantify the most abundant gangliosides from biological samples. CDs are potential tools for the analysis of lipids in both bioanalytical and biochemical applications, but their effects on gangliosides remain to be elucidated.

Therefore, the main objectives of this work were:

1. Development of a capillary electrophoresis method for the separation of the most abundant neuronal (GM1, GD1a, GD1b, GT1b and GQ1b) and peripheral (GM3) gangliosides.
    - Optimization of the separation and study the effect of various CDs.
    - Validation of the optimized method for the quantification of the major neuronal gangliosides from biological samples.
    - To demonstrate the applicability of the validated method on biological samples.
2. To investigate the effects of different CDs on ganglioside and cholesterol content of rat cerebral synaptosomes.
    - To elucidate the effects of two frequently used cholesterol extracting CDs on gangliosides: heptakis(2,6-di-O-methyl)-beta-cyclodextrin (DIMEB), which is a commercially available isomer of MBCD, and HPBCD.
    - To examine the applicability of ACD derivatives for selective extraction of gangliosides.
    - To examine the effects of the lipid extraction by CDs on synaptic glutamate release.

3. Methods

3.1. Chemicals

All reagents used in the experiments were analytical grade. Boric acid, sodium dodecyl sulfate (SDS), HEPES, sucrose, glucose, L-glutamate, L-cysteic acid, dimethyl sulfoxide (DMSO), octyl-β-D-thioglycopyranoside, sodium hydroxide (NaOH), 4-aminopyridine (4-AP) and other buffer components were purchased from Merck (Darmstadt, Germany). Fetal bovine serum (FBS) was obtained from Biosera (Nuaille, France). Methanol and chloroform used for LLE were purchased from Molar Chemicals Ltd. (Hungary). Ganglioside standards GM3, GM1, GD1a, GD1b, GT1b, GQ1b were products of Cayman Chemical Company (Ann Arbor, MI, USA). Alpha-cyclodextrin (ACD), beta-cyclodextrin (BCD), heptakis(2,6-di-O-methyl)-beta-cyclodextrin (DIMEB) with isomeric purity >35% DS~14, (2-hydroxypropyl)-beta-cyclodextrin (HPBCD) DS~4.5, randomly methylated alpha-cyclodextrin (RAMEA) DS~11 and (2-hydroxypropyl)-alpha-cyclodextrin (HPACD) DS~4.5 were purchased from Cyclolab Ltd. (Budapest, Hungary). 4-Fluoro-7-nitrobenzofurazan (NBD-F) was obtained from Tokyo Chemical Industry (Tokyo, Japan). DL-Threo-β-benzyloxyaspartic acid (DL-TBOA) was product of Tocris Bioscience (Bristol, United Kingdom). Ultrapure water was obtained from a Milli-Q Direct 8 System (Merck). The pH of the CE separation buffer was adjusted by 1 M NaOH solution.

3.2. Method optimization and validation of the CE method

3.2.1. Preparation of synaptosomes

Adult, male Wistar rats purchased from Toxi-Coop Ltd. (Budapest, Hungary) used for synaptosome preparation. Synaptosomes were prepared according to Modi and co-workers (108) with the following modifications. Animals were decapitated and the brain was removed rapidly. Isotonic sucrose buffer (0.32 M sucrose, 4 mM HEPES-NaOH, pH 7.4) was used to homogenize cerebrum and cerebellum with Potter S Homogenizer (B. Braun, Melsungen, Germany) with 15 strokes, at 1000 rpm. The homogenate was centrifuged (1500× *g*, 10 min, 4 °C) and the pellet was resuspended in sucrose buffer and centrifuged with the same parameters again. The two supernatants were combined and centrifuged (20,000× *g*, 30 min) to pellet the crude synaptosomes. The resulting supernatant was discarded and the pellet was washed again with an equal volume of

sucrose buffer and then pelleted by centrifugation (20,000× *g*, 30 min, 4 °C). Synaptosomes were stored frozen using cryopreservation buffer and slow freezing method (109, 110) to preserve their physiological state and integrity. Briefly, synaptosome pellets were resuspended in isotonic sucrose buffer containing 10% DMSO (*v/v*) and 10% FBS (*v/v*), and to slow down the freezing process at −80 °C, the samples were placed in a polystyrene box. Immediately prior to experiments, synaptosomes were rapidly thawed in a 37 °C water bath and pelleted by centrifugation (20 000× *g*, 10 min, 4 °C) to remove cryopreservation buffer. Then, the pellet was resuspended in isotonic HEPES-glucose buffer (10 mM HEPES-NaOH, 130 mM NaCl, 5.4 mM KCl, 1.3 mM $CaCl_2$, 0.9 mM $MgCl_2$, 5.5 mM glucose, pH 7.4) and aliquoted according to the experimental design.

3.2.2. Ganglioside extraction

Ganglioside samples were prepared by LLE method described by Svennerholm and Fredman (111), with minor modifications. Briefly, after thawing, synaptosomes were washed twice with 8 vol PBS to remove residual sucrose buffer which interfered with the electrophoretic separation of gangliosides. Ten mg synaptosomes (wet weight) was homogenized in 3 vol water with ultrasonic homogenizer (Labsonic 2000, B. Braun, Melsungen, Germany) for 10 s. Methanol (10.6 vol) containing the IS (72 nmol/mg wet weight) and the ganglioside standards, then chloroform (5.3 vol) was added to the homogenate. The mixture was vortexed briefly and pelleted by centrifugation (1000× *g*, 10 min, RT). The supernatant was collected and the pellet was re-extracted with chloroform-methanol-water (4:8:3, *v/v/v*). Then, the supernatants were combined to get a total lipid extract. It was mixed with water (0.173 vol) to induce solvent partitioning that resulted in a hydrophilic upper phase (U1) and a hydrophobic lower phase. The latter was then re-extracted with theoretical upper phase and the resulting upper phase (U2) was combined with U1. The combined upper phase was re-extracted with theoretical lower phase and the resulting ganglioside-containing upper phase was evaporated to dryness under a gentle stream of nitrogen (Zymark TurboVap LV, Hopkinton, MA, USA) in 37 °C water bath and stored at −20 °C until use.

For CE method validation, dry extracts yielded from 10 mg cerebral synaptosomes were resuspended in 60 μL water, centrifuged (20,000× *g*, 5 min, 4 °C) to remove precipitate and the supernatant was analyzed. Glass centrifuge tubes were used during the extraction in order to minimize sample loss by adsorption of gangliosides. For measuring the ganglioside content of cerebellar synaptosomes, dry ganglioside extracts were resuspended in 30 μL water.

3.2.3. Construction of calibration curves

Five-point calibration curves with four replicates were constructed for GM1, GD1a, GD1b, GT1b and GQ1b to cover the expected concentration range of study samples. Background subtraction method was used to prepare calibration curves. Calibrator samples were ganglioside extracts of rat cerebral synaptosomes spiked pre-extraction with standard solutions of the analytes. Zero calibrators spiked only with IS were used to obtain the background level of the analytes, which was subtracted from responses of spiked calibrator samples. The subtracted responses were then used to construct the calibration curves. For calculations, peak area ratios of analytes and IS were used. LOQ and LOD values were calculated according to ICH Q2B guidelines (112) by the following equations:

$$LOQ = 10\sigma/S \quad (1)$$

$$LOD = 3.3\sigma/S \quad (2)$$

where σ = the standard deviation of the Y-intercept and S = the slope of the calibration curve.

3.2.4. Precision and accuracy of the method

Quality control (QC) samples were analyzed to evaluate intraday and interday accuracy and precision across the quantification range. QC samples were measured in three independent runs of separate days, in four replicates. Similarly to calibrators, pre-spiked rat cerebral synaptosome samples were used as QC samples. Three added concentration levels of each ganglioside were used for the preparation of QC samples. QC samples were analyzed against the calibration curve and the concentrations obtained were compared with nominal value. Accuracy was given as percent of the nominal value. Precision was

calculated as relative standard error of the measurements. Accuracy was accepted within ± 15% of the nominal value, except the lowest QC level, where ± 20% was accepted. Precision was accepted within ± 15% RSD, except the lowest QC level, where ± 20% RSD was accepted.

3.2.5. Extraction recovery of analytes

Extraction recovery was determined by analyzing QC samples at three concentration levels on three separate days in four replicates. Recovery was calculated as follows: pre-extraction spiked sample/post-extraction spiked sample*100. RSDs of the recoveries determined on three separate days was used to express the reproducibility of extraction efficiency, which was acceptable within ± 15% RSD, except at the lowest QC level, where ± 20% was accepted.

3.2.6. Stability of the lipid extract

Stability of the samples was evaluated at different storage conditions by analyzing QC samples at three concentration levels, in four replicates. To assess autosampler stability, evaporated samples dissolved in water were analyzed after storage at 5 °C for 24 hours. For evaluation of long-term stability, evaporated samples were stored at −20 °C for 1 week, then dissolved in water and were measured. A deviation of less than ± 15% from the nominal concentration was acceptable.

3.2.7. Instrumentation

Ganglioside analysis was performed on a P/ACE MDQ capillary electrophoresis system with UV-VIS detection (200 nm) operated by 32 Karat software version 5.0 (Beckman Coulter Inc., Brea, CA, USA). Uncoated fused silica capillaries with 75 µm internal diameter were used (Agilent Technologies, Santa Clara, CA, USA). The first conditioning of the capillary was carried out by rinsing with 1 M NaOH solution (60 psi, 30 min), 0.1 M NaOH solution (60 psi, 30 min) and then ultrapure water (60 psi, 30 min). The capillary was flushed with 0.5% SDS (60 psi, 2 min) and separation buffer (60 psi, 3 min) between runs. The separation buffers were degassed in an ultrasonic bath for 5 minutes before use. The temperatures of the capillary cartridge and the autosampler unit were maintained at 15 °C and 5 °C, respectively. Constant voltage was applied during the separation, which

was investigated in the range of +10-25 kV. The samples were introduced into the capillary by hydrodynamic injection (0.5 psi, 5 s). Gangliosides were identified by spiking the biological samples with analytical standards.

3.3. Studying the effects of CDs on synaptosomes

3.3.1. Incubation of synaptosomes with CDs

For all types of experiments, except glutamate release measurements, rat cerebral synaptosomes were incubated for 40 min at 37 °C in 500 µL HEPES-glucose buffer with or without CDs, resulting in vehicle-treated (control) and CD-treated synaptosomes, respectively. CD solutions contained DIMEB, HPBCD, RAMEA or HPACD in various concentrations (0.3-100 mM). After incubation, synaptosomes were pelleted by centrifugation (20,000× *g*, 5 min, 4 °C) and used immediately for further analysis. The slightly different incubation method used in glutamate release measurements is described in the corresponding section. Osmolarities of CD solutions were adjusted and they were between 290 and 310 mOsm.

3.3.2. Ganglioside analysis

For CD-treatments, ganglioside levels of rat cerebral synaptosomes were determined by the validated CE method with the optimum separation parameters described in the following sections.

3.3.3. Cholesterol assay

Cholesterol levels of rat cerebral synaptosomes were analyzed with Cholesterol Fluorometric Assay Kit (Cayman Chemical Company, Ann Arbor, MI, USA) with minor adjustments for sample preparation. Briefly, after CD treatments, 2 mg of synaptosomes were extracted with 10 vol chloroform-methanol 2:1 (*v/v*) to gain a lipid extract. The samples were centrifuged (20,000× *g*, 5 min, 4 °C) and the supernatant was evaporated to dryness under nitrogen stream in 37 °C water bath (Zymark TurboVap LV). The extracts were reconstituted and diluted in assay buffer (1.2 mL/mg synaptosome). Further preparation of the assay was done according to the manufacturer's protocol. Fluorescence was measured with a Varioskan LUX multimode microplate reader (Thermo Fisher Scientific, Waltham, MA, USA) at 530/590 nm. Cholesterol depletion in CD-treated

synaptosomes was calculated as the percentage of cholesterol content of vehicle-treated synaptosomes.

3.3.4. Resazurin reduction viability assay

Viability of rat cerebral synaptosomes was measured by Resazurin Cell Viability Kit (Cell Signaling Technology Inc., Danvers, MA, USA) with minor modifications. The assay is based on the reduction of nonfluorescent resazurin by intracellular dehydrogenase enzymes to highly fluorescent resorufin. After CD treatments, 2 mg of synaptosomes were centrifuged (20,000× *g*, 5 min, 4 °C) and the supernatant was discarded. The synaptosome pellet was then gently resuspended in HEPES-glucose buffer (pH 7.4) containing 10% resazurin solution. After 25 min incubation, synaptosomes were pelleted by centrifugation (20,000× *g*, 5 min, 4 °C). The fluorescence of the supernatant was measured with a Varioskan LUX multimode microplate reader (Thermo Fisher Scientific) at 530/590 nm. Viability of CD-treated synaptosomes was calculated as the percentage of vehicle-treated control synaptosomes.

3.3.5. Membrane integrity measurement by LDH release assay

Membrane integrity of synaptosomes was measured by CytoTox-ONE Homogeneous Membrane Integrity Assay (Promega, Madison, WI, USA) with minor modifications. The assay measures the release of lactate dehydrogenase (LDH) enzyme from synaptosomes with damaged membrane.

Briefly, after CD treatments, 2 mg of synaptosomes were centrifuged (20,000× *g*, 5 min, 4 °C) and the supernatant was collected to measure LDH release from synaptosomes. To determine the total LDH content, the synaptosome pellet was lysed with 1% Triton X-100 solution (*v/v*). Both supernatant and lysis samples were diluted 10-fold. LDH activity was then assessed according to the manufacturer's instructions. The fluorescence was measured by Varioskan LUX multimode microplate reader (Thermo Fisher Scientific) at 530/590 nm. The LDH release from synaptosomes was calculated as percentage of total LDH content determined by Triton X-100 lysis.

3.3.6. Glutamate release measurement

After thawing and centrifugation, the cryopreserved synaptosomes were resuspended in isotonic HEPES-glucose buffer. Synaptosomal suspensions corresponding to 10 mg of synaptosomes were centrifuged to an 8-well strip plate (15 min, 2500× *g*, 4 °C) and the supernatant was discarded. Vehicle-treated (control) and CD-treated synaptosomes were incubated for 40 min at 37 °C in 200 µL HEPES-glucose buffer with or without CDs, respectively. CD solutions contained 10 mM DIMEB, 34 mM HPBCD, 26 mM RAMEA or 85 mM HPACD. After incubation, the supernatant was replaced with fresh HEPES-glucose buffer containing 40 µM DL-TBOA (a competitive, non-transportable blocker of excitatory amino acid transporters that inhibits the reuptake of released glutamate (113)). Then, synaptosomes were equilibrated for 2×10 min at 37 °C with buffer replacement. After equilibration, the buffer was replaced by fresh HEPES-glucose buffer in case of non-stimulated groups. To evoke depolarization, the buffer was replaced by HEPES-glucose buffer containing 1 mM 4-AP. Following stimulation, aliquots were taken from the buffer at 8 min and stored at −20 °C until CE analysis.

Glutamate content of aliquots was analyzed by a CE-LIF method developed in our laboratory (114). Briefly, samples were derivatized with NBD-F (1 mg/mL final concentration) in 20 mM borate buffer, pH 8.5 for 20 min at 65 °C. 1 µM L-Cysteic acid was used as internal standard. Derivatized samples were analyzed by a P/ACE MDQ Plus capillary electrophoresis system (SCIEX, Framingham, MA, USA) equipped with a laser source of excitation and emission wavelengths of 488 and 520 nm, respectively. Separation was carried out in polyacrylamide-coated fused silica capillaries with 75 µm internal diameter, 10 and 50 cm effective and total capillary length, respectively (Agilent Technologies). The separation electrolyte contained 8 mM BCD and 100 mM sodium borate at pH 8.5. Glutamate release was normalized to the baseline release from vehicle-treated, unstimulated synaptosomes.

3.4. Statistical analysis

Data were analyzed by GraphPad Prism 8 (GraphPad Software, La Jolla, CA, USA). Simple linear regression was used for construction of calibration curves of gangliosides.

Ganglioside contents of cerebrum and cerebellum were compared by Student's unpaired t-test.

In depletion studies, IC_{50} values were determined from concentration-response curves constructed by non-linear regression method. In glutamate release experiments, one-way ANOVA followed by Bonferroni's *post hoc* test was used for data analysis. All data are presented as means ± SEM of at least three parallel measurements. Differences were considered significant if $p < 0.05$.

4. Results

4.1. Optimization of separation conditions

CE separations were carried out in uncoated fused silica capillaries. At neutral to alkaline pH, gangliosides have one or more negative charge, depending on the number of sialic acids attached to the oligosaccharide chain, and have electromigration towards the anode. In this pH range, the magnitude of electroosmotic flow (EOF) was considerably stronger than the electrophoretic mobility of the negatively charged analytes, thus gangliosides migrated towards the cathode.

4.1.1. Effects of various CDs on the separation of gangliosides

Based on the observations on the crucial role of ACD in the separation of gangliosides (80, 81), we investigated the effect of various CDs as buffer additives on the separation of GM3, GM1, GD1a, GD1b, GT1b and GQ1b standards. CDs were tested in various concentration ranges while keeping sodium borate concentration (100 mM), pH of the electrolyte (pH 10.0) and other separation conditions (+25 kV voltage, 70 cm effective capillary length) constant.

The effect of cavity size on the separation were investigated by using native ACD, BCD and GCD. First, we tested native ACD, which is considered to have optimal cavity size for complexation with long saturated alkyl chains. It was tested in the concentration range of 5-40 mM. ACD at 15 mM concentration provided separation between gangliosides containing different numbers of sialic acid. At concentrations higher than 15 mM ACD no further improvement in the resolution was observed, on the contrary, the baseline noise increased. However, only partial resolution was achieved between the two monosialogangliosides (GM3 and GM1), as they migrated as overlapping double peaks (Figure 3A). Similarly, only partial resolution was obtained between the two disialogangliosides (GD1a and GD1b) too.

DOI:10.14753/SE.2023.2805

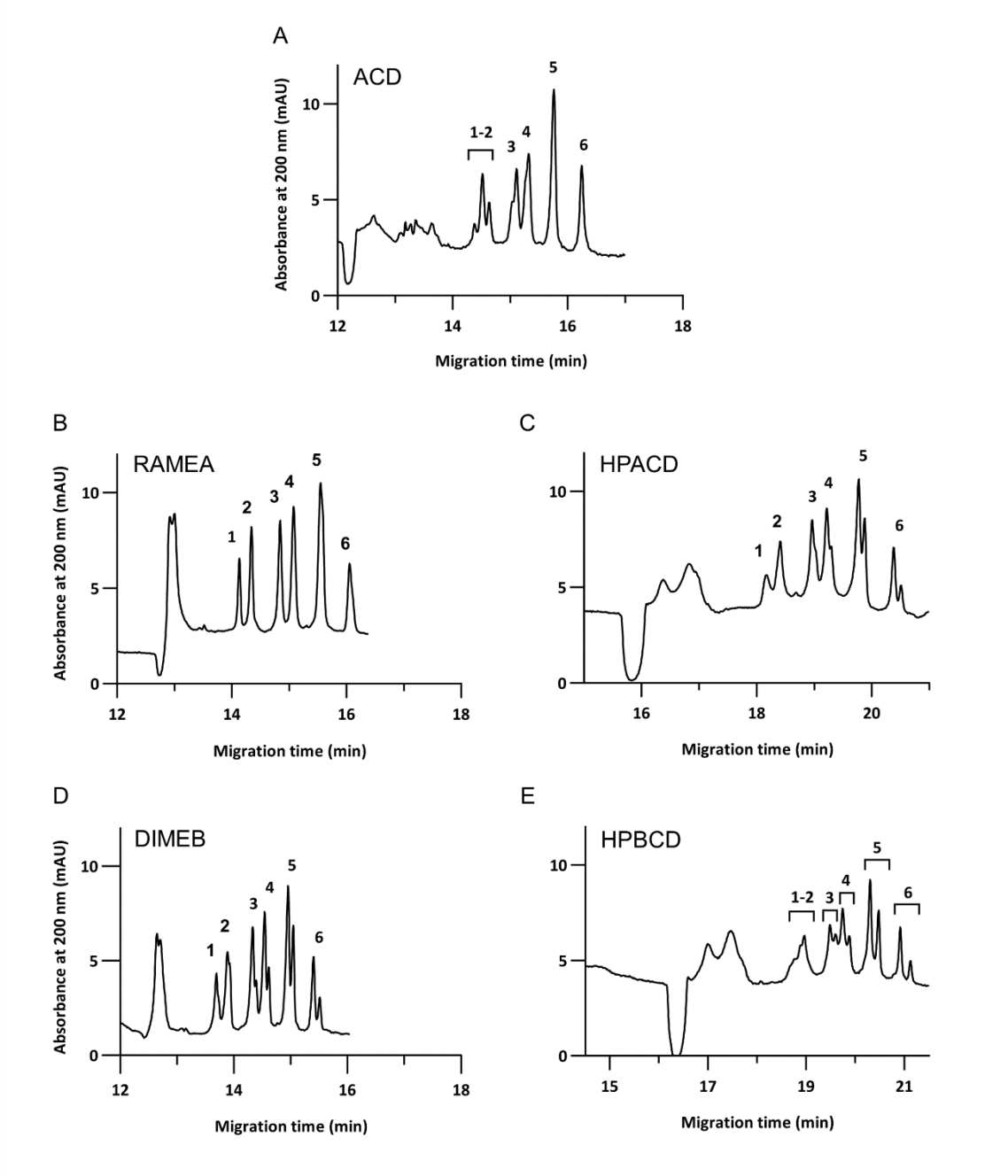

Figure 3. Separation of standard mixture of gangliosides with 15 mM ACD (**A**), 20 mM RAMEA (**B**), 90 mM HPACD (**C**), 15 mM DIMEB (**D**) and HPBCD (**E**) as additive in 100 mM sodium borate buffer, pH 10.0. Voltage: +25 kV; temperature: 15 °C; capillary: 70/80 cm×75µm i.d. uncoated fused silica capillary. 1: GM3; 2: GM1; 3: GD1a; 4: GD1b; 5: GT1b; 6: GQ1b (13).

Native BCD (5-15 mM) and GCD (5-30 mM) were also examined as buffer additives, however they had negligible effect on the separation of the tested gangliosides.

DOI:10.14753/SE.2023.2805

Derivatives of ACD and BCD were also investigated. The effect of RAMEA on the separation of gangliosides was tested in the concentration range of 5-30 mM. Figure 4 shows that RAMEA at 5 mM concentration initiates separation between the mono-, di-, tri- and tetrasialogangliosides. Further increase in RAMEA concentration resulted in baseline separation of all six gangliosides with slight increase in migration times. Splitting peaks were observed in the range of 5-15 mM RAMEA, while above this concentration single peaks were obtained. Above 20 mM RAMEA, no further improvement in the separation was achieved (Figure 3B).

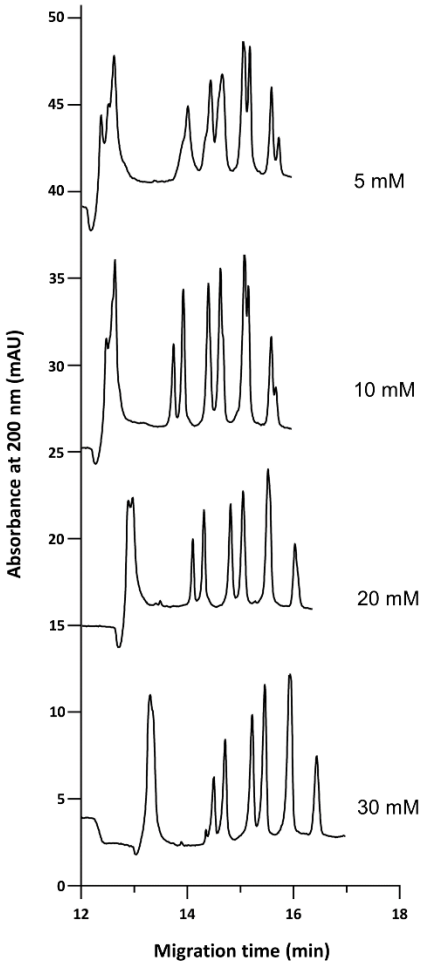

Figure 4. Separation of standard mixture of gangliosides in the presence of various concentrations of RAMEA as additive in 100 mM sodium borate buffer, pH 10.0. Other separation conditions are as in Figure 3. Peaks in order of migration: GM3; GM1; GD1a; GD1b; GT1b; GQ1b.

HPACD was examined in the concentration range of 5-90 mM. Figure 3C shows that HPACD provided separation between gangliosides with different number of sialic acids. However, even at the highest examined, 90 mM concentration, only partial resolution was observed between GM3-GM1 and between GD1a-GD1b, while the analysis time increased considerably. Peak splitting was observed, similarly to ACD.

We investigated the influence of two BCD derivatives with high water solubility on the separation of gangliosides. DIMEB was tested in the concentration range of 5-30 mM, where separation between the mono-, di-, tri- and tetrasialogangliosides was observed. The application of DIMEB in the separation buffer resulted in the partial resolution between GM3 and GM1, and between GD1a-GD1b. Furthermore, splitting peaks were obtained, as shown in Figure 3D. Above 15 mM DIMEB, no further improvement was obtained in the separation.

We also tested the effect on the separation of HPBCD in the concentration range of 5-90 mM and separation of the mono-, di-, tri- and tetrasialogangliosides was also observed, although at very high, 90 mM concentration (Figure 3E). Similarly to HPACD, only partial resolution of gangliosides with the same number of sialic acid was obtained that accompanied with long migration times and broad peaks.

4.1.2. Effects of sodium borate concentration and pH on the separation of gangliosides

The effect of sodium borate concentration was examined at pH 10.0 in the presence of 20 mM RAMEA, while keeping other separation conditions (+25 kV voltage, 70 cm effective capillary length) constant. We investigated the effect of sodium borate in the concentration range of 50-150 mM (Figure 5). With increasing borate concentration, EOF decreased and an increase in ganglioside migration time was observed. At 100 mM borate appropriate separation of all six gangliosides was obtained. Further increasing the borate concentration resulted in peak broadening and production of significant amount of Joule heat.

DOI:10.14753/SE.2023.2805

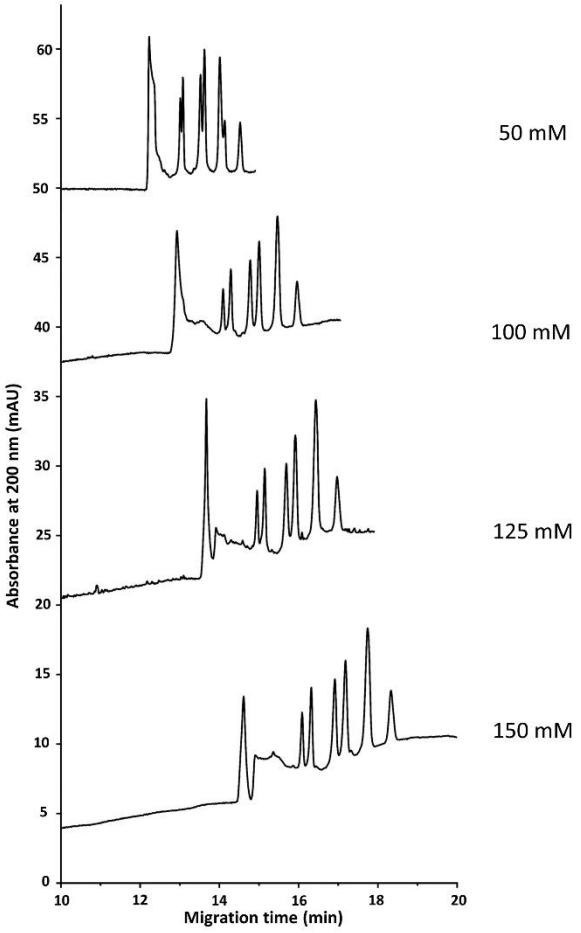

Figure 5. Separation of standard mixture of gangliosides in the presence of various concentrations of sodium borate at pH 10.0 with 20 mM RAMEA as additive. Other separation conditions are as in Figure 3. Peaks in order of migration: GM3; GM1; GD1a; GD1b; GT1b; GQ1b.

The effect of the pH of the sodium borate buffer was tested at 100 mM borate concentration in the presence of 20 mM RAMEA, in a 70 cm effective length capillary by applying +25 kV voltage. Since borate has a pK_a value of 9.14, the examined pH range was 8.5-10.0, where sufficient buffer capacity could be obtained. At more alkaline pH, where the ionization of borate is more effective, improved resolution of the analytes was observed. As Figure 6 shows, at the lowest examined value, pH 8.5, no separation between GM3 and GM1, and only partial resolution of the disialoganglioside isomers

were obtained. Increasing pH value resulted in improving resolution of the analytes, and at pH 10.0, acceptable resolution of all six gangliosides was obtained.

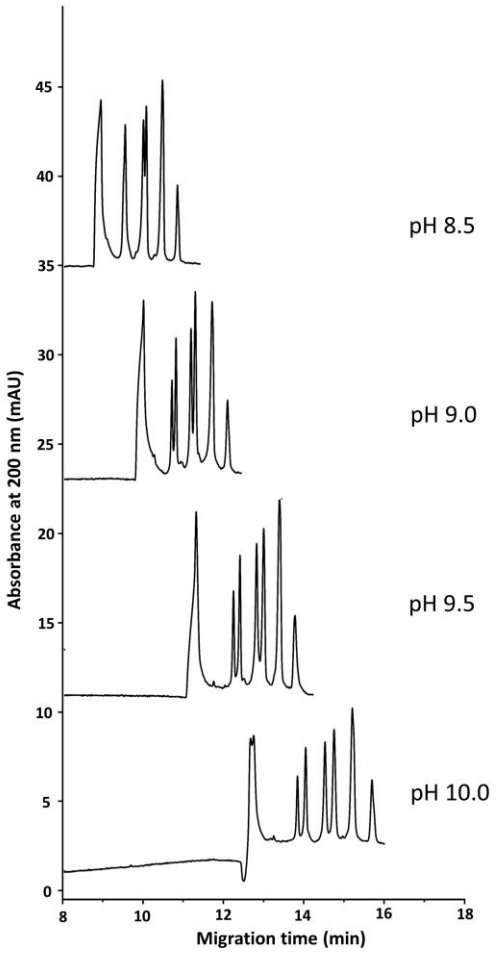

Figure 6. Separation of standard mixture of gangliosides at various pH values in 100 mM sodium borate buffer with 20 mM RAMEA as additive. Other separation conditions are as in Figure 3. Peaks in order of migration: GM3; GM1; GD1a; GD1b; GT1b; GQ1b.

As Figure 7 shows, increasing either the sodium borate concentration or pH level resulted in the increase in relative migration times of GM1 and GD1b, compared to GM3 and GD1a, respectively.

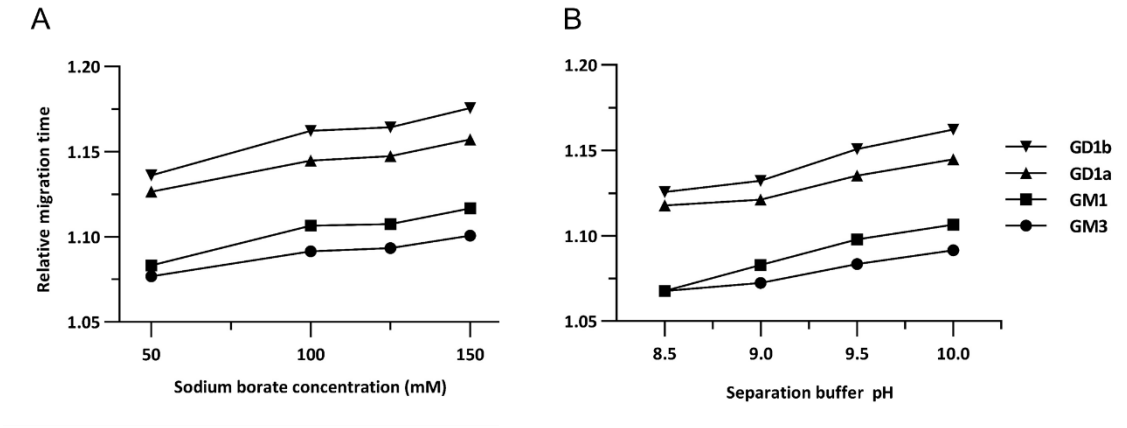

Figure 7. Effect of sodium borate concentration (**A**) and pH (**B**) on relative migration times of gangliosides. Other separation conditions are as in Figure 3. The relative migration times are ratios of migration times of analytes and EOF (13).

4.1.3. Other separation conditions

Other separation parameters were also investigated using a separation buffer containing 20 mM RAMEA, 100 mM sodium borate at pH 10.0. Different capillary lengths were tested, where 80 cm total and 70 cm effective capillary length was found to be necessary to obtain resolution between the analytes. The effect of the applied voltage was tested in the range of +10-25 kV, where the application of +25 kV voltage resulted in the highest separation efficiency and shorter migration times. Capillary temperature was kept at 15°C in order to eliminate Joule heating and subsequent formation of temperature gradients and band broadening.

The biological samples were analyzed dissolving dry ganglioside extracts in different solvents: 100% methanol, methanol-water 1:1 (*v/v*) and 100% water were tested. It was found that the presence of methanol in the solution is not suitable, because of the higher evaporation rate of the low volume sample (60 µL) even using thermostated sample tray. The autosampler temperature was kept at 5 °C in order to minimize sample evaporation and improve sample stability.

Decreased EOF and increased analysis time were observed in the analysis of biological samples, probably due to the effect of residual protein content, which was eliminated by

a short centrifugation step before sample injection and by washing the capillary with 0.5% SDS solution.

4.2. Results of method validation

The final composition of the separation buffer chosen for the validation were 100 mM sodium borate at pH 10.0 with 20 mM RAMEA as additive, and an applied voltage of +25 kV. For method validation, ganglioside extracts of rat cerebral synaptosome samples were used. Figure 8 shows a representative electropherogram of the samples.

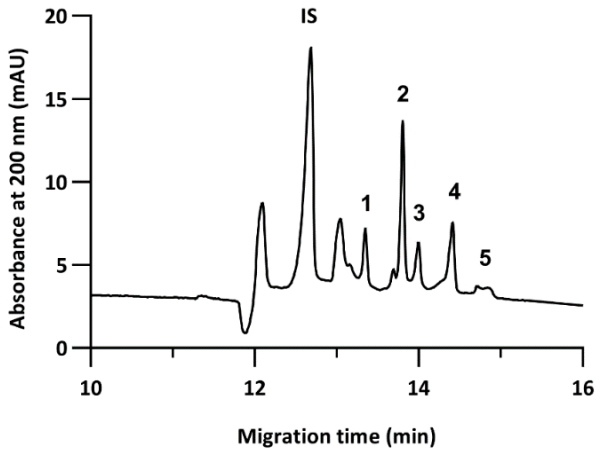

Figure 8. Electropherogram of ganglioside extract of rat cerebral synaptosomes. Separation buffer: 100 mM sodium borate, pH 10.0, 20 mM RAMEA. Other separation conditions are as in Figure 3. 1: GM1; 2: GD1a; 3: GD1b; 4: GT1b; 5: GQ1b; IS: internal standard (13).

First, several substances were tested as potential internal standards (IS). Octyl-β-D-thioglycopyranoside, a nonionic surfactant was selected as during sample extraction it partitions into the aqueous phase along with gangliosides. Furthermore, it has a shorter migration time than gangliosides have at the optimum separation conditions. No interfering peaks were observed at the migration time of the IS.

The regression coefficients (R^2) of the calibration curves of each ganglioside were higher than 0.995 confirming linear relationship between peak area ratios and concentrations in the calibration range (Table 1). LOQ and LOD values were between 16.8-97.1 μM and 5.2–32.0 μM, respectively (Table 1).

Table 1. Validation parameters of linearity, LOD and LOQ of the optimized method (13).

Gangliosides	GM1	GD1a	GD1b	GT1b	GQ1b
Linear range (µM)	40-200	100-350	35-125	40-200	5-20
Slope	2.14E-03	2.83E-03	2.68E-03	4.32E-03	4.81E-03
Standard error of slope	3.04E-05	1.21E-04	9.73E-05	5.42E-05	1.15E-04
Y-intercept	1.35E-02	3.84E-02	2.40E-02	4.93E-02	1.78E-02
Standard error of Y-intercept	3.82E-03	2.75E-02	8.14E-03	6.81E-03	1.46E-03
Regression coefficient (R^2)	0.9994	0.9945	0.9960	0.9995	0.9983
LOD (µM)	5.9	32.0	10.0	5.2	1.0
LOQ (µM)	17.9	97.1	30.4	15.8	3.0

Interday and intraday precision and accuracy were within the acceptable range as shown in Table 2. Extraction recoveries determined at low, medium and high concentration levels were higher than 85% for each analyte, with an RSD of less than 13% (Table 2).

DOI:10.14753/SE.2023.2805

Table 2. Intra- and interday precision, accuracy and recovery of the optimized method (13).

	Added concentration (µM)	Intraday (n=4)			Interday (n=3)			Recovery (n=3)	
		Mean (µM)	Precision (%RSD)	Accuracy (%)	Mean (µM)	Precision (%RSD)	Accuracy (%)	Mean (%)	%RSD
GM1	40	39.4	7.38	98.6	40.4	7.23	100.9	102.4	9.07
	70	68.8	8.69	98.3	64.3	6.26	91.8	99.0	6.16
	150	127.7	5.64	85.1	126.7	3.60	85.5	85.7	1.76
GD1a	100	110.0	9.74	110.0	104.2	5.94	104.2	109.1	3.75
	150	158.4	8.29	105.6	154.7	2.20	103.1	115.7	4.29
	200	187.5	7.24	93.7	189.7	8.15	94.9	90.8	4.63
GD1b	35	30.9	5.06	88.2	33.2	7.03	94.9	108.3	8.02
	75	68.5	12.14	91.4	69.8	7.97	93.1	108.9	11.93
	100	97.6	4.26	97.6	94.0	5.36	94.0	100.3	0.74
GT1b	40	44.2	7.47	110.5	45.3	3.74	113.4	101.6	5.28
	70	72.2	9.27	103.2	68.3	7.67	97.5	106.0	10.30
	150	132.8	3.71	88.6	133.4	3.55	88.9	85.5	3.03
GQ1b	5	4.7	8.59	96.8	5.5	10.93	110.8	110.3	12.22
	10	10.3	10.61	100.5	9.8	2.30	97.9	90.2	4.81
	15	14.1	7.52	91.1	14.2	5.68	95.0	107.0	8.91

For autosampler stability, samples stored at 5 °C were found stable for at least 24 h with accuracy values of 89–113% and RSDs of less than 11%. Long-term stability samples were stored at −20 °C for one week before determination of their ganglioside concentrations that were within 88–112% with less than 10% RSDs.

The applicability of the method to biological samples was demonstrated by analysis of ganglioside extracts from rat cerebral and cerebellar synaptosomes. We identified the major neuronal gangliosides (GM1, GD1a, GD1b, GT1b and GQ1b) in both brain areas. Their levels are shown in Table 3. Total ganglioside concentration of cerebral synaptosomes was found to be approximately five times higher than that in cerebellum.

Table 3. Tissue ganglioside concentrations in rat cerebral and cerebellar synaptosomes (13).

	Tissue ganglioside concentration (nmol/g wet weight)	
	Cerebral synaptosome	**Cerebellar synaptosome**
GM1	283 ± 46	28 ± 6
GD1a	716 ± 136	92 ± 13
GD1b	138 ± 55	23 ± 6
GT1b	375 ± 44	124 ± 11
GQ1b	109 ± 10	34 ± 3
Total	1621 ± 278	302 ± 17

The values are means±SD (n=3-5).

The percent distribution of individual gangliosides compared to the total content were calculated for cerebral and cerebellar synaptosomes (Figure 9). We found that, the main components in both brain areas were GD1a and GT1b constituting about 70% of the total amount. The most abundant ganglioside was, however GD1a (44%) in cerebrum and GT1b (41%) in cerebellum. Significant differences were found between the two sample types in the contribution of GM1, GD1a, GT1b and GQ1b.

DOI:10.14753/SE.2023.2805

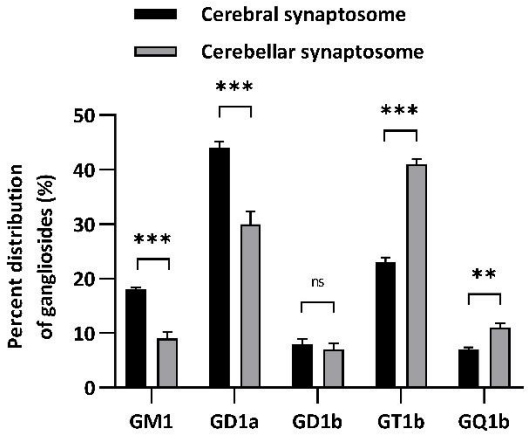

Figure 9. Comparison of ganglioside patterns in rat cerebral and cerebellar synaptosomes. Values are means±SEM (n=3-5) and are expressed as percentage of total gangliosides. Student's t test was used to compare individual gangliosides between the two brain areas. ***p≤0.001, **p≤0.01, ns: not significant (13).

4.3. Effects of CDs on ganglioside and cholesterol content of synaptosomes

Ganglioside and cholesterol depleting effects of DIMEB, HPBCD, RAMEA and HPACD were investigated by incubating rat cerebral synaptosomes in CD solutions of different concentrations and then analyzing their residual ganglioside and cholesterol content.

It was found that DIMEB potently depleted both cholesterol and gangliosides from synaptosomes, in a similar concentration range. Estimated IC_{50} values were 7.4 mM and 10.5 mM for cholesterol and ganglioside extraction, respectively. We did not identify a selective concentration range for cholesterol extraction, and at a DIMEB concentration of 60 mM, we observed almost complete depletion of both lipids (Figure 10A).

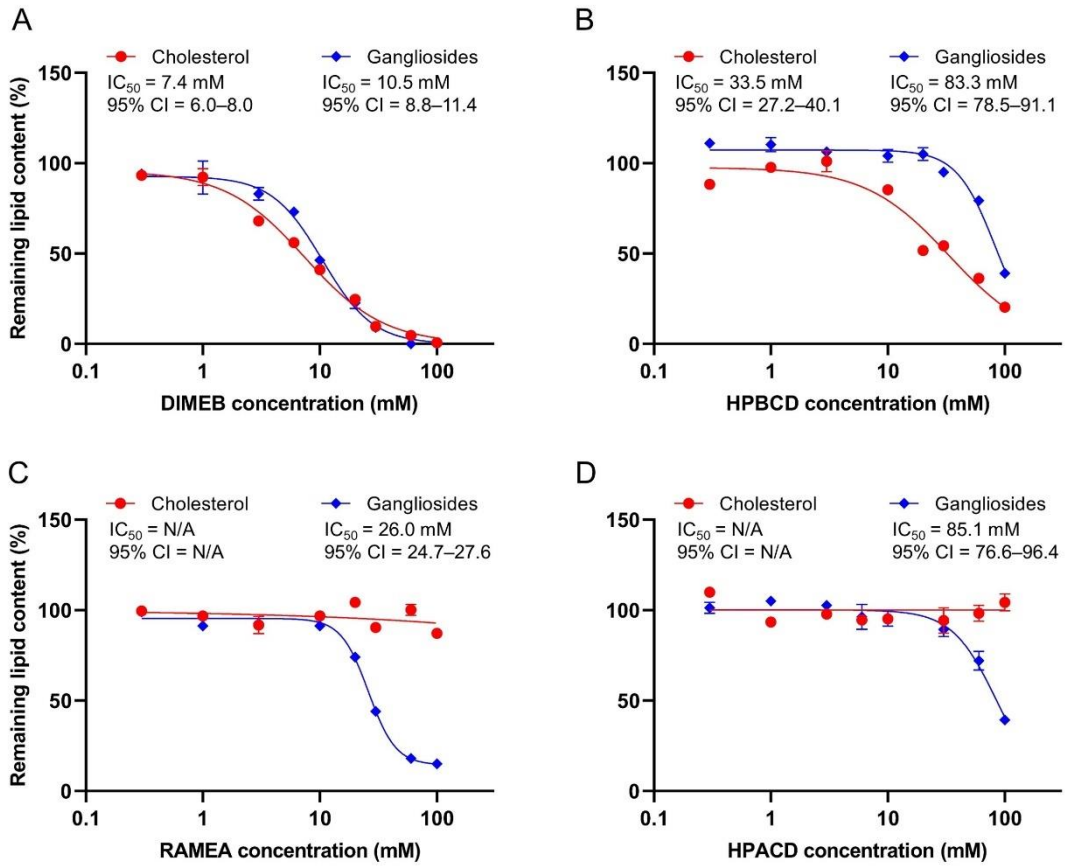

Figure 10. Effect of DIMEB (**A**), HPBCD (**B**), RAMEA (**C**), HPACD (**D**) on ganglioside and cholesterol content of rat cerebral synaptosomes. Lipid levels were measured after 40 min exposure of synaptosomes to cyclodextrins. Values are expressed as the percentage of untreated synaptosomes. IC_{50} values and their 95% confidence intervals (95% CI) are given. Data are represented as means ± SEM (n=3). N/A means non applicable (115).

We found that HPBCD also depleted both cholesterol (IC_{50} = 33.5 mM) and gangliosides (IC_{50} = 83.3 mM), but less potently, than DIMEB did (Figure 10B). However, in contrast to DIMEB, HPBCD showed a significant difference in cholesterol and ganglioside depleting ability, with negligible ganglioside loss (~5%) at 50% cholesterol depleting concentration.

No considerable cholesterol reduction in synaptosomes was observed with ACD derivatives in the studied concentration range (Figure 10C and 10D). On the other hand, both derivatives reduced ganglioside levels. RAMEA was found to be more potent (IC_{50}

= 26.0 mM) than HPACD (IC_{50} = 85.1 mM), the latter causing only ~60% reduction at the highest examined, 100 mM concentration.

Concentration-response curves were constructed for depletion of individual neuronal gangliosides, however no reasonable difference was found in individual IC_{50} values for any CD derivatives tested (Table 4). Therefore, depletion of total ganglioside content is shown in the lipid depletion curves in Figure 10.

Table 4. IC_{50} values and their 95% confidence intervals (95% CI) of depletion of individual and total ganglioside content upon DIMEB, HPBCD, RAMEA and HPACD treatment of rat cerebral synaptosomes (115).

	DIMEB		HPBCD		RAMEA		HPACD	
	IC_{50} (mM)	95% CI	IC_{50} (mM)	95% CI	IC_{50} (mM)	95% CI	IC_{50} (mM)	95% CI
GM1	15.0	12.7–17.6	80.8	76.0–89.5	29.1	27.9–30.5	86.7	79.0–100.7
GD1a	9.7	7.3–15.0	83.7	78.6–90.4	25.1	23.4–27.2	72.9	65.6–82.7
GD1b	14.5	10.7–23.9	86.6	80.2–98.0	26.4	24.6–28.3	90.6	68.2–139.9
GT1b	8.7	7.9–9.6	80.1	74.6–90.5	24.2	22.8–25.6	104.8	93.9–133.5
GQ1b	11.4	9.8–13.4	85.1	71.3–105.0	30.3	26.3–42.0	61.2	45.5–72.2
Total	10.5	8.8–11.4	83.3	78.5–91.1	26.0	24.7–27.6	85.1	76.6–96.4

Depletion of individual neuronal gangliosides (GM1, GD1a, GD1b, GT1b, GQ1b) is shown. Total ganglioside levels are given as sum of individual ganglioside ones. Values were estimated by concentration-response nonlinear fitting.

4.4. Effects of CDs on the membrane integrity and viability of synaptosomes

Concentration dependent increase of LDH release with an IC_{50} value of 18.3 mM was observed upon DIMEB treatment in cerebral synaptosomes. Interestingly, the extent of membrane integrity loss reached a plateau at ~60% LDH release (Figure 11A). At the same time, significant decrease in metabolic activity was measured at concentrations higher than 10 mM. The estimated IC_{50} value of viability loss was 26.5 mM and total loss of viability was seen at 60 mM DIMEB concentration (Figure 11A).

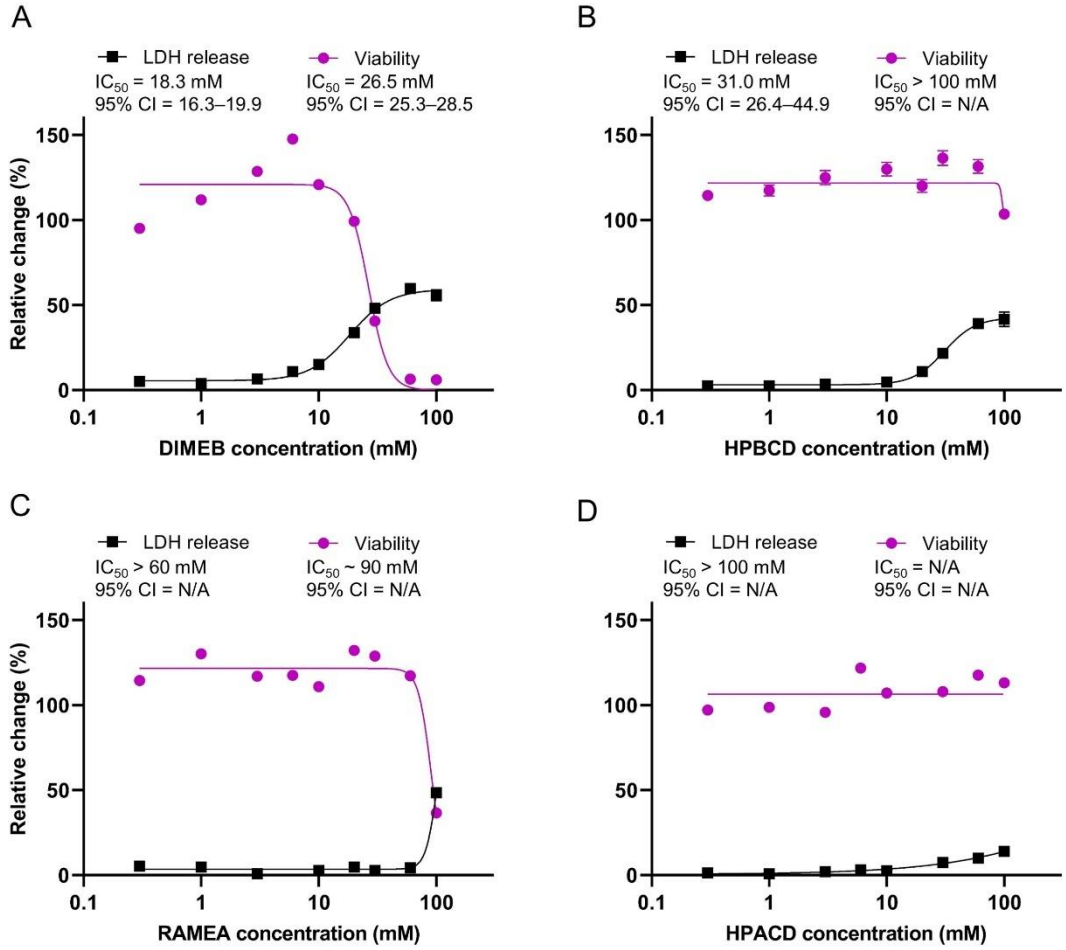

Figure 11. Effect of DIMEB (**A**), HPBCD (**B**), RAMEA (**C**), HPACD (**D**) on membrane integrity and viability of rat cerebral synaptosomes. Synaptosomes were analyzed after 40 min exposure to cyclodextrins. For estimating membrane integrity, LDH release from synaptosomes was calculated as percentage of total LDH content determined by Triton X-100 lysis. Viability was measured by resazurin reduction assay and values are expressed as the percentage of untreated synaptosomes. IC_{50} values and their 95% confidence intervals (95% CI) are given. Data are represented as means ± SEM (n=3). N/A means non applicable (115).

HPBCD induced membrane damage at higher concentration than DIMEB, with an IC_{50} value of 31.0 mM (Figure 11B) and had a similar maximal effect of 43% LDH release. Likewise, HPBCD decreased viability only at the highest examined, 100 mM concentration.

The examined ACD derivatives induced less damage in synaptosomal membranes than the BCD derivatives did. Decreased membrane integrity and viability was observed only

at the highest tested, 100 mM concentration of RAMEA (Figure 11C). HPACD caused mild increase in LDH release and had no effect on viability even at the highest tested concentration (Figure 11D).

4.5. Effects of CDs on glutamate release from synaptosomes

We treated rat cerebral synaptosomes with DIMEB, HPBCD, RAMEA or HPACD to examine the effect of lipid depletion on glutamate release. Selective ganglioside depletion was induced with the use of RAMEA and HPACD at their 50% ganglioside depleting concentrations (26 mM and 85 mM, respectively). Selective cholesterol depletion was obtained by treatment with 33 mM HPBCD, where 50% cholesterol and negligible ganglioside extraction was measured in the previous experiments. Treatment of synaptosomes with 10 mM DIMEB induced about 50% ganglioside and cholesterol extraction. Following CD-treatments, we determined basal (non-stimulated) and 4-aminopyridine (4-AP)-evoked glutamate release from synaptosomes.

All four CDs significantly increased basal glutamate release from synaptosomes (Figure 12). Interestingly, stimulated glutamate release was not detected in the RAMEA, HPACD and DIMEB-treated groups, where depletion of gangliosides was induced. In contrast, in the HPBCD-treated synaptosomes, where cholesterol was selectively depleted, 4-AP stimulation still induced glutamate release, similarly to the untreated groups.

DOI:10.14753/SE.2023.2805

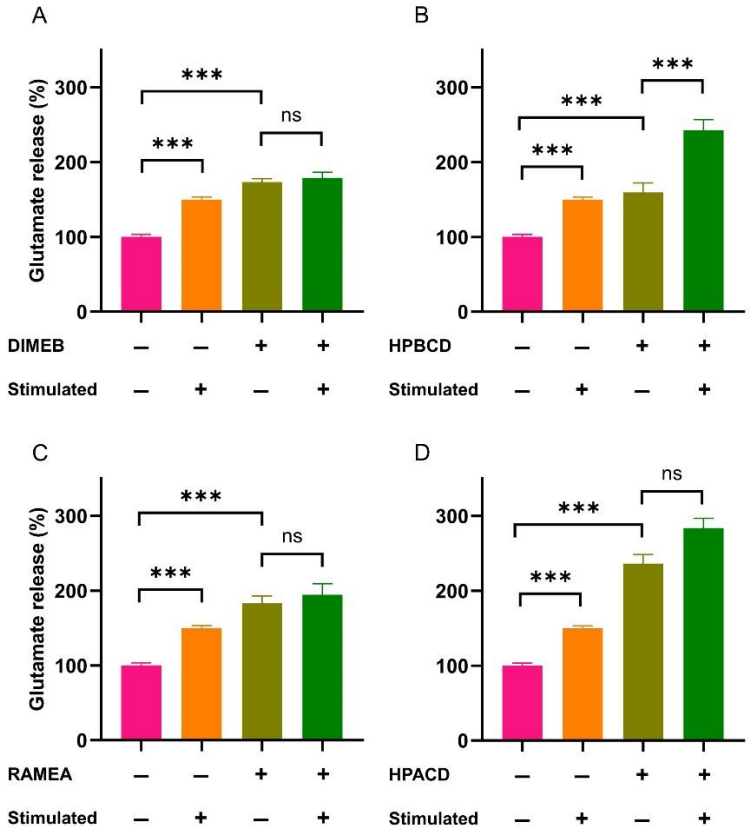

Figure 12. Basal (non-stimulated) and 4-aminopyridine-evoked release of glutamate from rat cerebral synaptosomes upon DIMEB (**A**), HPBCD (**B**), RAMEA (**C**), HPACD (**D**) treatment. Glutamate release were measured after 40 min exposure of synaptosomes to cyclodextrins. Glutamate release is expressed as the percentage of baseline release from untreated synaptosomes. Data are represented as means±SEM (n=8). One-way ANOVA followed by Bonferroni's *post hoc* test was used for data evaluation. ***$p \leq 0.001$, ns: not significant (115).

5. Discussion

5.1. Optimization of separation conditions

CE is an attractive separation technique, as it offers high separation efficiency, low-volume sample requirement and short analysis time. It is also a versatile technique, since the same instrument can be used to separate a wide range of analytes. Another advantage of CE is that separation selectivity can be changed by using different buffer additives, such as cyclodextrins or ion pairing agents that can alter – among others – the electrophoretic mobility of analytes.

CE has been applied for the analysis of lipids, however there are several difficulties to overcome, such as the low aqueous solubility and poor UV absorbance of lipids (116). Aqueous separation buffers have been applied to resolve relatively less hydrophobic lipids with C2-C14 chain length without any additive (117). However, the increasing alkyl chain length has been shown to cause several analytical difficulties, such as decreasing analyte solubility, micelle formation and decreasing selectivity, therefore the separation of most lipids with >C17 requires MEKC or the application of organic solvents in the separation buffer (116).

Gangliosides also have several physicochemical properties that make their CE separation challenging. As previous studies have shown they form micelles or mixed micelles in aqueous solutions (78) that hinders their separation as monomers (80). Besides, gangliosides with the same number of sialic acids have a relatively small difference in their charge-to-mass ratios, e.g., GM1 has only two more neutral monosaccharides in the carbohydrate chain than GM3. Furthermore, the two structural isomers, GD1a and GD1b, differ only in the position of the terminal sialic acid and therefore have same charge and molecular weight.

Although several CE methods have been developed for the separation of gangliosides, validated method for their quantitative analysis from biological samples were not reported. It was previously shown that using alkaline borate buffer with ACD as additive, separation of standards of major neuronal gangliosides (GM1, GD1a, GD1b, GT1b) was be achieved with CE (80-82). Neuronal tetrasialoganglioside GQ1b, with relevance in neurotransmitter release (49, 55) was not investigated in these studies. Besides, data on

the CE separation of underivatized GM3, the most abundant peripheral ganglioside, were also not available, however, GM3 can be found together with GM1 in insulin-sensitive tissues (25, 27-29), therefore their separation is necessary in order to study ganglioside-related mechanisms in these tissues by CE. Based on these literature data, our initial investigations focused on the separation of the most abundant neuronal (GM1, GD1a, GD1b, GT1b, GQ1b) and extraneural (GM3) gangliosides.

5.1.1. Effects of various CDs on the separation of gangliosides

Over the past three decades, CDs have been extensively used in CE methods as chiral selectors, mainly for the enantioseparation of drugs or other biologically relevant compounds such as amino acids. In addition to their chiral recognition ability, CDs are efficient lipid solubilizers, therefore their use as buffer additives in CE methods can be advantageous in lipid analysis. Improvement in analyte solubility and increased separation efficiency was observed with the application of CDs for the separation of fatty acids (117, 118).

As it was mentioned above, CDs have also been used in the separation of gangliosides. The separation observed with ACD was considered to be the effect of disruption of ganglioside micelles through complex formation (80, 81). In the case of gangliosides, it can be assumed that the fatty acid and sphingosine of the ceramide moiety are involved in the complexation with CDs, based on their capability to solubilize fatty acids. However, direct evidence for the complex formation has not yet been provided.

Without any additives, we did not observe separation of the individual gangliosides and they migrated as one broad peak in the aqueous electrolyte with high electrophoretic mobility, presumably in micellar form. The reduced migration time observed when CDs were used in the separation buffer was considered as an indicator of micelle disruption and the formation of inclusion complexes, as complex formation results in a decrease in the charge-to-mass ratio of the analytes and hence a decrease in electrophoretic mobility.

The cavity size of the CD ring has been shown to be a major factor for inclusion complex formation with lipids (99). Thus, we investigated the effect of native CDs with different cavity sizes on the separation of the six, most abundant gangliosides. Using native ACD

as a buffer additive, gangliosides with different number of sialic acid could be separated, however, our results showed that ACD does not provide sufficient resolution between the two monosialogangliosides as they migrated as overlapping double peaks. Therefore, ACD was considered unsuitable for quantitative determination and consequently this CD was excluded from further method development.

Since BCDs are also known to form stable complexes with long-chain fatty acids (103), we tested the effect of native BCD on the separation. In the examined concentration range, which was limited due to its poor water solubility (<18 mM), however, we did not obtain separation. Likewise, native GCD had practically no effect on the separation, which was in accordance with our expectations since the cavity size of GCD is too wide, and therefore the least favorable to form stable complex with the saturated alkyl chains of gangliosides. In line with our results, GCDs were reported as the least effective CD to solubilize fatty acids (99). Our results with native BCD and GCD are also consistent with previous separation attempts using CE (80, 81).

In our further investigations, we tested derivatives of ACD and BCD. Previous studies showed that besides that the cavity size of CDs, the type of the substituents also have strong impact of the complexation (103). Despite we obtained no separation of gangliosides with the use of native BCD, we examined its methylated and hydroxypropylated derivatives with higher aqueous solubility. Similarly, methylated and hydroxypropylated derivatives of ACD were examined. All four CD derivatives (DIMEB, HPBCD, RAMEA and HPACD) were able to separate gangliosides with different number of sialic acids, but significant differences were found in the separation pattern and effective concentration range.

We examined the effect of RAMEA, which is a mixture of methylated ACDs at random positions, with an average of 12-14 methyl groups on the CD ring. RAMEA in the separation buffer effectively disrupted ganglioside micelles and at 20 mM concentration, it provided separation between gangliosides according to the difference in their oligosaccharide chain. In detail, GM3 and GM1 was successfully separated and acceptable resolution between GD1a and GD1b isomers was achieved.

We also examined the effect of DIMEB on the separation. DIMEB is a single isomer, with 14 methyl groups in a CD molecule, at C2 and C6 positions. Similarly to RAMEA, using DIMEB in the electrolyte resulted in separation between GM3 and GM1, however in this case splitting peaks of the individual gangliosides were obtained in the tested concentration range.

Based on the electropherograms, both hydroxypropylated derivatives, HPACD and HPBCD, were able to form complexes with gangliosides. They shared similarities in their separation properties indicating a significant involvement of the hydroxypropyl groups in the complex formation. Hydroxypropylated derivatives induced ganglioside micelle disruption at higher concentrations than RAMEA or DIMEB, suggesting that the stability of hydroxypropylated-CD/ganglioside complexes is lower than that of the methylated derivatives. These results are in line with previous observations that hydroxypropylated derivatives are of lower lipid solubilizing capacity than methylated ones (101-103). The hydroxypropyl groups provide elongated cavity, however they are less hydrophobic and bulkier than the methyl groups, and the steric hindrance at high degree of substitution could also contribute to its lower lipid solubilization capacity (99, 119). Based on molecular dynamic simulations, the 2-hydroxypropyl groups located at the O2 positions widen the CD cavity at the secondary face, but are spatially more spread out and dynamically more restricted, due to the formation of a hydrogen bond network between the OH groups of the side chains and the glucose units (120). Due to the high concentration of hydroxypropylated CDs, the viscosity of the CE separation buffer increased significantly, resulting in long analysis times. Therefore, the use of these CDs for the CE separation of gangliosides proved to less appropriate.

The double peaks of individual ganglioside standards observed with several CDs presumably represent their different lipoforms since they are mixtures of gangliosides with C18:1 and C20:1 sphingoid backbones according to the manufacturer. It is known that the molar ratio of CDs to fatty acids is affected by the alkyl chain length. For example, Ishiguro observed that linoleic and eicosapentaenoic acid (C18:2 and C20:5, respectively) form complexes with 1–2 and 3–4 CDs, respectively (121). Therefore, double peaks could be explained by different complex formation stoichiometry or stability with C18:1 and C20:1 sphingosines, resulting in their partial separation appearing double peaks if the

difference between the charge-to-mass ratio or the stability of the complexes is high enough.

To summarize, while the cavity diameter of ACDs is considered to be optimal for complexing long saturated alkyl chains, our studies with CE suggests that methylated and hydroxypropylated derivatives of BCD can also form complexes with gangliosides. We found that the type of the substituents had a strong influence on the separation pattern, presumably as a consequence of their complexation ability. Based on our and literature data, we can suspect two distinct mechanisms being involved in CE separation of gangliosides in the presence of CDs. Gangliosides form micelles and mixed micelles in the aqueous separation buffer, so the electrophoretic mobility of each ganglioside species is indistinguishable. Complexation with CDs, however, disrupts the micelles and facilitates the separation of individual ganglioside species according to the difference of their own electrophoretic mobility. This mechanism is presumably the basis of the separation of glycoforms. In case of lipoforms, however, complexes with different stoichiometry or stability can be formed, which is the likely reason of their separation.

Since our primary objective was to separate the different ganglioside glycoforms, RAMEA had the advantage over the other CDs tested as it provided single peaks and less complex electropherograms by avoiding discrimination between ganglioside lipoforms. Furthermore, all six tested gangliosides were separated with acceptable resolution and analysis time, therefore, for further separation studies RAMEA was chosen.

5.1.2. Effects of sodium borate concentration and pH on the separation of gangliosides

Borate buffers are extensively used in CE separations at alkaline pH. Due to their low mobility, borate anions produce low current and Joule heating during separation, which are advantageous for both resolution and analyte stability. Borate buffers exhibit low UV background absorbance, which is also useful for the separation of gangliosides characterized by weak chromophore property. Another well-known property of borate is that it forms stable complexes with cis-diols and this property is exploited in many CE methods, for example in the analysis of neutral carbohydrates (122-124), nucleotides (125, 126), or phenolic compounds (127). Upon complexation with borate at alkaline pH,

the additional negative charge on the analyte provides alteration in its electrophoretic mobility. This can be particularly advantageous in the resolution of analytes like gangliosides having only small differences in their charge-to-mass ratio. Interaction of borate with 1,2-cis-diols give the most stable complex, however, complex formation with 1,3-cis-diols can also occur (128, 129). On the oligosaccharide chain of gangliosides, free hydroxyl groups at C3-C4 and C4-C6 positions on terminal galactose or GalNAc are assumed to be possible sites for complexation with borate (122, 130).

We investigated the effect of sodium borate concentration in the range of 50-150 mM, at pH 10.0, where the monovalent borate anion $B(OH)_4^-$ dominates. The observed increased relative migration times and improving separation upon increasing sodium borate concentration was probably the effect of decreasing EOF and the higher extent of borate complexation with free hydroxyl groups of the oligosaccharide chain of gangliosides. Similar improvement in the separation was seen with increasing pH, where the ionization of boric acid is more effective. The observed difference in the relative migration times of GM1 and GD1b, compared to GM3 and GD1a respectively, can be the result of the complex formation of the free C3-C4 hydroxyl groups on their terminal galactose units with borate.

As a result, 100 mM sodium borate at pH 10.0 was selected as a good compromise for high resolution, acceptable analysis times and current.

5.2. Method validation

Gangliosides are endogenous compounds, therefore, due to the lack of analyte-free biological samples, background subtraction method was used to assess accuracy and precision and to construct calibration curves, taking into account ICH guidelines in method validation strategies for endogenous compounds (131). The endogenous background level of a given ganglioside was subtracted from the level obtained from the pre-spiked samples. With this method, the same sample matrix can be used for calibrators, QC samples and study samples, avoiding any difference in sample recovery or matrix effect. However, a limitation of this method is that the increase of the background peak area has to be significantly higher than the reproducibility of the method, therefore at least 15-20% increase in background responses is needed (132). The relatively high LOQ and

LOD values of our method are thus the consequence of the endogenous background levels, and do not represent the real analytical sensitivity of the CE method, and lower concentrations might also be detected.

Comparing the sensitivity of our CE method to those of the most commonly used TLC methods is difficult, since in this case sensitivity is obtained in LBSA content, instead of concentrations of individual gangliosides. Nevertheless, the reported 0.15 µg LOQ of LBSA (64) corresponds to approximately one order of magnitude higher ganglioside concentration than the limit of quantification of our CE method. However, the nM-range sensitivity of the reported LC-MS methods (72-74) exceeds that of our methods.

Results of interday and intraday accuracy and precision indicated that the closeness of repeated measurement results to the true value, as well as to each other are within the acceptable range.

As our method employed a sample extraction step, recovery (extraction efficiency) was evaluated. Recovery values of the analytes indicated good reproducibility of the sample extraction procedure.

Based on the results of stability measurements, ganglioside extracts dissolved in water can be stored at 5 °C for at least 24 h without stability problems and dry ganglioside extracts are stable at least for one week, stored at −20 °C.

Compared to the other mentioned analytical techniques, our CE method requires fewer sample preparation steps, as it offers acceptable sensitivity without derivatization and purification of gangliosides. For other separation techniques, DEAE-chromatography, solid phase extraction or dialysis may be necessary in order to eliminate small polar or uncharged molecules, proteins or free fatty acids that may partition into the aqueous phase of LLE (59, 62).

The established method was found suitable for application on biological samples. The measured ganglioside levels and percent distribution values are comparable with those reported by other authors for brain homogenates (24, 25).

5.3. Effects of CDs on the ganglioside and cholesterol content of synaptosomes

Methylated BCDs are extensively used as cholesterol-depleting agents, but their selectivity over other lipids is not fully characterized. Ottico and co-workers (105) studied the effect of MBCD treatment on rat cerebellar granule cells, where reduction on sphingomyelin and GSL levels in addition to cholesterol depletion was observed. In line with these results, we observed considerable ganglioside depleting capability of DIMEB. Thus, biological effect of MBCDs observed in other studies are cannot be explained by cholesterol removal alone, as they may also interact with other membrane components, among which gangliosides play prominent role in protein regulation.

Our results showed that another extensively used BCD derivative, HPBCD is not entirely selective for cholesterol, but in an appropriate concentration range, the selective extraction can be achieved. Its inferior potency compared to methylated BCDs in terms of cholesterol depletion was previously shown by other authors (104, 105), which is in line with our present results. The lower cholesterol depleting capacity of HPBCD is probably the reason why it is less frequently used in *in vitro* studies. In addition, its effects on other membrane components have hardly been investigated, however, it was revealed in a study on its potential mechanism in NPC that it lowers accumulation of GM3 and GM2 immunoreactivity in a mouse model of the disease (133).

In our studies, ACD derivatives with smaller cavity size were not able to extract cholesterol from cerebral synaptosomes, which result is line with literature data (100, 134, 135). Relatively few data are available on the effects of ACD or its derivatives on other membrane components too. In previous studies, where the interaction of native ACD with other membrane constituents was examined, depletion of phospholipids was reported (134, 135). In terms of ACD derivatives, it was found that both DIMEA (hexakis(2,6-di-O-methyl)-alpha-cyclodextrin) and HPACD lowered lysosomal accumulation of GM1 immunofluorescence in a cell model of GM1 gangliosidosis, and similarly to our results, the methylated derivative of ACD was more effective (136). In the study of Davidson and co-workers (133), HPACD was found to be much less effective than HPBCD in reducing GM2 and GM3 ganglioside immunoreactivity accumulation.

5.4. Effects of CDs on the membrane integrity and viability of synaptosomes

Since we observed significant changes in the membrane lipid composition of cerebral synaptosomes upon CD treatment, we investigated whether they have an effect on membrane integrity and viability. Release of cytosolic LDH enzyme was used to estimate impaired membrane integrity and the reduction of resazurin by metabolically active synaptosomes was used to assess viability.

Our results on the effect on membrane integrity and viability are in accordance with previous reports on cells suggesting that cholesterol depletion has a major impact on membrane damage and reduced viability (104, 135). The hypothesis that toxic effect of CDs highly depends on their cholesterol lowering capacity is supported by the correlation observed between cholesterol complexation and cytotoxicity, as well as hemolytic activity (137, 138). ACDs that are unable complexing cholesterol (102), also induced some damage in our experiments, that might be explained by their interaction with other membrane constituents such as phospholipids (135) in high concentrations.

Our results are in accordance with previous observations that methylated derivatives among both ACDs and BCDs are the most toxic. Methylated BCDs were found to induce hemolysis in lower concentrations than other BCD derivatives (137, 139). Similar tendency on their cytotoxic effect was reported by many authors using various cell lines (137, 140-142). Likewise, methylated ACD derivatives were found to be the most toxic in a recent study (143).

In our experiments, LDH release assay that is commonly used to measure the extent of cell death, showed enhanced membrane permeability rather than direct toxicity since lipid depletion even at 100 mM CD concentration did not induce total membrane integrity loss. The complete loss of viability measured by resazurin reduction assay upon DIMEB treatment, however, is probably due to the massive leakage of small molecules that are essential for normal metabolic activity. In accordance, Ottico and co-workers (105) reported that while MBCD treatment considerably increased membrane permeability, the MTT assay showed a smaller decrease in the viability of cerebellar granule cells. These findings that LDH release is not a true estimate of cytotoxicity in case of CD-treatments,

where alterations in the composition of plasma membrane are induced. Therefore, a complementary assay is also required to assess changes in metabolic activity.

5.5. Effects of CDs on glutamate release from synaptosomes

Although the involvement of cholesterol in regulating of the release of neurotransmitters from synapses was investigated by several research groups (144, 145), the possible role of gangliosides has remained mainly unexplored. Therefore, we treated rat cerebral synaptosomes with DIMEB, HPBCD, RAMEA or HPACD to reveal whether lipid depletion has an effect on glutamate release. CDs were used at concentrations where they had no effect on viability and only minor effect on membrane integrity.

The measured increased basal release of glutamate may be the consequence of the mildly impaired membranes of synaptosomes resulting in a steady leakage of the neurotransmitter. Our results also suggest that stimulated glutamate release is dependent on the ganglioside rather than cholesterol content of synaptic membranes.

It was shown previously that several proteins, involved in exocytosis are localized in membrane microdomains, such as syntaxin and SNAP-25 (146, 147) voltage-gated Ca^{2+} and K^{+} channels (148-150). To investigate the localization of these proteins, mainly MBCD was used to deplete cholesterol to induce the disruption of membrane microdomains. In line with our results, it was reported that MBCD treatment impaired the exocytotic release of glutamate from rat brain synaptosomes (151, 152) and that of dopamine from PC12 cells (146). The effect of MBCD treatment was mostly explained as a result of the lowered cholesterol levels in the membrane. However, we showed that DIMEB extracts gangliosides to a similar extent as cholesterol. This suggests that the reported effects of MBCD treatments cannot be attributed solely to cholesterol removal.

The involvement of gangliosides in neurotransmitter release was investigated by the direct modulation of gangliosides too. It was observed that exogenous administration of GM1 and GQ1b enhanced the depolarization-evoked Ca^{2+}-influx and release of acetylcholine from rat brain synaptosomes (49). Elevated intracellular Ca^{2+} concentration, which is a prerequisite step of neurotransmission, was also measured upon depolarization in GM1-treated PC12 cells, where dihydropyridine-sensitive calcium

channels were found to be influenced by the increased concentration of GM1 (48). Furthermore, the inhibition of ganglioside synthesis was also shown to decrease glutamate release from neuro2a neuroblastoma cell line (50, 51), confirming the role of gangliosides in neurotransmitter release.

In line with these reports, we found reduced depolarization-evoked glutamate release only when ganglioside depletion was induced, but not upon selective cholesterol depletion.

DOI:10.14753/SE.2023.2805

6. Conclusions

Based on our separation experiments with CE and literature data, it can be assumed that the tested hydroxypropylated and methylated ACD and BCD derivatives are able to disrupt ganglioside micelles by complex formation. It can be concluded that RAMEA is suitable for the separation of the most abundant gangliosides (GM3, GM1, GD1a, GD1b, GT1b, GQ1b) under the optimal separation conditions, since separation according to the glycan part can be achieved. The observed increase in the relative migration times of GM1 and GD1b during separation in alkaline sodium borate buffer indicates that complexation occurs between borate and the oligosaccharide chain of gangliosides, resulting in additional negative charge.

The examined CD derivatives were able to extract gangliosides from the plasma membrane as well. We have seen that DIMEB extracts gangliosides to a similar extent as cholesterol, so the biological effects of methylated BCDs commonly used as cholesterol depleting agents cannot be explained solely by cholesterol removal. Considering the role of gangliosides in the regulation of several membrane proteins, this interaction should be taken into account, when interpreting the results of MBCD treatments. We also suggest that HPBCD may be more appropriate for selective cholesterol depletion due to the difference in the IC_{50} values of ganglioside and cholesterol depletion and its lower toxicity. We propose that the tested ACD derivatives, RAMEA and HPACD, could be used as ganglioside extracting tools to manipulate their plasma membrane content.

The applicability of the tested CD derivatives to modify membrane lipid composition was demonstrated by investigating their influence on glutamate release from rat cerebral synaptosomes to reveal whether lipid depletion has an effect on synaptic activity. The results suggest that glutamate release is more dependent on ganglioside rather than cholesterol content of the membrane. Further studies are needed to clarify the exact role of gangliosides in neurotransmitter release.

DOI:10.14753/SE.2023.2805

7. Summary

Gangliosides are glycosphingolipids of the plasma membrane and are highly abundant in the nervous system, where they play a vital role in normal cell functions. Besides, several studies suggest that altered ganglioside levels contribute to the pathogenesis of neurological conditions. Due to their importance, efficient analytical methods are necessary to determine individual gangliosides in biological samples. CDs are efficient lipid solubilizers and, based on their specific interactions with lipids, CDs with different cavity sizes and substituents may be applied in various bioanalytical and biochemical experiments as selective lipid recognizing tools.

In our work, a CE method has been optimized and validated for the quantification of neuronal gangliosides (GM1, GD1a, GD1b, GT1b and GQ1b). The most abundant extraneural ganglioside, GM3 can also be separated by this method. Native and substituted CDs were tested as buffer additives in order to disrupt ganglioside micelles in the aqueous separation buffer. The presence of borate was found to be essential for the separation of gangliosides with the same number of sialic acids. The best resolution was observed using 20 mM RAMEA in alkaline sodium borate buffer enabling the separation of the examined gangliosides according to their oligosaccharide chain. The applicability of the validated method has been demonstrated by the quantification of gangliosides from rat cerebral and cerebellar synaptosomes.

Despite CDs are known to interact with membrane lipids, their effect on gangliosides is poorly characterized. Methylated BCDs are commonly used as selective cholesterol-depleting agents, but we showed that DIMEB also extracts gangliosides from rat brain synaptosomes in a similar concentration range. Based on our results, HPBCD is more suitable for selective cholesterol depletion, due to the significant difference in its cholesterol and ganglioside extracting concentrations. The two tested ACD derivatives, RAMEA and HPACD were able to extract gangliosides without affecting cholesterol content, therefore they may be appropriate for their selective depletion. Ganglioside, but not cholesterol depletion interfered with depolarization-evoked glutamate release from rat brain synaptosomes, indicating that stimulated neurotransmitter release is more dependent on ganglioside rather than cholesterol content. Our results emphasize the significance of gangliosides in different membrane functions and the importance of the characterization of lipid depleting capacity of different CDs.

8. References

1. Sastry PS. (1985) Lipids of Nervous-Tissue - Composition and Metabolism. Progress in Lipid Research, 24: 69-176.
2. Sipione S, Monyror J, Galleguillos D, Steinberg N, Kadam V. (2020) Gangliosides in the Brain: Physiology, Pathophysiology and Therapeutic Applications. Frontiers in Neuroscience, 14.
3. Sonnino S, Mauri L, Chigorno V, Prinetti A. (2007) Gangliosides as components of lipid membrane domains. Glycobiology, 17: 1R-13R.
4. Todeschini AR, Hakomori SI. (2008) Functional role of glycosphingolipids and gangliosides in control of cell adhesion, motility, and growth, through glycosynaptic microdomains. Biochimica Et Biophysica Acta-General Subjects, 1780: 421-433.
5. Lopez PHH, Schnaar RL. (2009) Gangliosides in cell recognition and membrane protein regulation. Current Opinion in Structural Biology, 19: 549-557.
6. Yu RK, Tsai YT, Ariga T, Yanagisawa M. (2011) Structures, biosynthesis, and functions of gangliosides--an overview. J Oleo Sci, 60: 537-544.
7. Sonnino S, Chigorno V. (2000) Ganglioside molecular species containing C18- and C20-sphingosine in mammalian nervous tissues and neuronal cell cultures. Biochim Biophys Acta, 1469: 63-77.
8. Kolter T. (2012) Ganglioside biochemistry. ISRN Biochem, 2012: 506160.
9. Chiricozzi E, Di Biase E, Lunghi G, Fazzari M, Loberto N, Aureli M, Mauri L, Sonnino S. (2021) Turning the spotlight on the oligosaccharide chain of GM1 ganglioside. Glycoconjugate Journal, 38: 101-117.
10. Svennerholm L. (1994) Designation and Schematic Structure of Gangliosides and Allied Glycosphingolipids. Biological Function of Gangliosides, 101: R11-R14.
11. Schnaar RL, Lopez PHH. (2018) Preface and Ganglioside Nomenclature. Gangliosides in Health and Disease, 156: Xvii-Xxi.
12. Sonnino S, Chiricozzi E, Grassi S, Mauri L, Prioni S, Prinetti A. (2018) Gangliosides in Membrane Organization. Prog Mol Biol Transl Sci, 156: 83-120.
13. Geda O, Tabi T, Szoko E. (2021) Development and validation of capillary electrophoresis method for quantification of gangliosides in brain synaptosomes. J Pharm Biomed Anal, 205: 114329.

14. Quinn PJ, Wolf C. (2009) The liquid-ordered phase in membranes. Biochim Biophys Acta, 1788: 33-46.
15. Gupta G, Surolia A. (2010) Glycosphingolipids in microdomain formation and their spatial organization. FEBS Lett, 584: 1634-1641.
16. Munro S. (2003) Lipid rafts: Elusive or illusive? Cell, 115: 377-388.
17. Sevcsik E, Schutz GJ. (2016) With or without rafts? Alternative views on cell membranes. Bioessays, 38: 129-139.
18. Westerlund B, Slotte JP. (2009) How the molecular features of glycosphingolipids affect domain formation in fluid membranes. Biochim Biophys Acta, 1788: 194-201.
19. Bach D, Sela B, Miller IR. (1982) Compositional aspects of lipid hydration. Chemistry and Physics of Lipids, 31: 381-394.
20. Kwak DH, Seo BB, Chang KT, Choo YK. (2011) Roles of gangliosides in mouse embryogenesis and embryonic stem cell differentiation. Exp Mol Med, 43: 379-388.
21. Yu RK, Bieberich E, Xia T, Zeng G. (2004) Regulation of ganglioside biosynthesis in the nervous system. Journal of Lipid Research, 45: 783-793.
22. Yamashita T, Wada R, Sasaki T, Deng C, Bierfreund U, Sandhoff K, Proia RL. (1999) A vital role for glycosphingolipid synthesis during development and differentiation. Proc Natl Acad Sci U S A, 96: 9142-9147.
23. Jennemann R, Sandhoff R, Wang S, Kiss E, Gretz N, Zuliani C, Martin-Villalba A, Jager R, Schorle H, Kenzelmann M, Bonrouhi M, Wiegandt H, Grone HJ. (2005) Cell-specific deletion of glucosylceramide synthase in brain leads to severe neural defects after birth. Proc Natl Acad Sci U S A, 102: 12459-12464.
24. Tettamanti G, Bonali F, Marchesini S, Zambotti V. (1973) A new procedure for the extraction, purification and fractionation of brain gangliosides. Biochim Biophys Acta, 296: 160-170.
25. Iwamori M, Shimomura J, Tsuyuhara S, Nagai Y. (1984) Gangliosides of various rat tissues: distribution of ganglio-N-tetraose-containing gangliosides and tissue-characteristic composition of gangliosides. J Biochem, 95: 761-770.
26. Prokazova NV, Samovilova NN, Gracheva EV, Golovanova NK. (2009) Ganglioside GM3 and its biological functions. Biochemistry (Mosc), 74: 235-249.

27. Sanchez SS, Abregu AV, Aybar MJ, Sanchez Riera AN. (2000) Changes in liver gangliosides in streptozotocin-induced diabetic rats. Cell Biol Int, 24: 897-904.
28. Svennerholm L, Bruce A, Mansson JE, Rynmark BM, Vanier MT. (1972) Sphinolipids of human skeletal muscle. Biochim Biophys Acta, 280: 626-636.
29. Lopez PHH, Aja S, Aoki K, Seldin MM, Lei X, Ronnett GV, Wong GW, Schnaar RL. (2017) Mice lacking sialyltransferase ST3Gal-II develop late-onset obesity and insulin resistance. Glycobiology, 27: 129-139.
30. Svennerholm L, Bostrom K, Jungbjer B, Olsson L. (1994) Membrane lipids of adult human brain: lipid composition of frontal and temporal lobe in subjects of age 20 to 100 years. J Neurochem, 63: 1802-1811.
31. Vajn K, Viljetic B, Degmecic IV, Schnaar RL, Heffer M. (2013) Differential Distribution of Major Brain Gangliosides in the Adult Mouse Central Nervous System. Plos One, 8.
32. Ma Q, Kobayashi M, Sugiura M, Ozaki N, Nishio K, Shiraishi Y, Furukawa K, Furukawa K, Sugiura Y. (2003) Morphological study of disordered myelination and the degeneration of nerve fibers in the spinal cord of mice lacking complex gangliosides. Arch Histol Cytol, 66: 37-44.
33. Sheikh KA, Sun J, Liu Y, Kawai H, Crawford TO, Proia RL, Griffin JW, Schnaar RL. (1999) Mice lacking complex gangliosides develop Wallerian degeneration and myelination defects. Proc Natl Acad Sci U S A, 96: 7532-7537.
34. Collins BE, Ito H, Sawada N, Ishida H, Kiso M, Schnaar RL. (1999) Enhanced binding of the neural siglecs, myelin-associated glycoprotein and Schwann cell myelin protein, to Chol-1 (alpha-series) gangliosides and novel sulfated Chol-1 analogs. J Biol Chem, 274: 37637-37643.
35. Lee MC, Lee WS, Park CS, Juhng SW. (1994) The biologic role of ganglioside in neuronal differentiation--effects of GM1 ganglioside on human neuroblastoma SH-SY5Y cells. J Korean Med Sci, 9: 179-187.
36. Roisen FJ, Bartfeld H, Nagele R, Yorke G. (1981) Ganglioside stimulation of axonal sprouting in vitro. Science, 214: 577-578.
37. Da Silva JS, Hasegawa T, Miyagi T, Dotti CG, Abad-Rodriguez J. (2005) Asymmetric membrane ganglioside sialidase activity specifies axonal fate. Nat Neurosci, 8: 606-615.

38. Lunghi G, Fazzari M, Di Biase E, Mauri L, Sonnino S, Chiricozzi E. (2020) Modulation of calcium signaling depends on the oligosaccharide of GM1 in Neuro2a mouse neuroblastoma cells. Glycoconjugate Journal, 37: 713-727.
39. Schengrund CL. (2010) Lipid rafts: keys to neurodegeneration. Brain Res Bull, 82: 7-17.
40. de Chaves EP, Sipione S. (2010) Sphingolipids and gangliosides of the nervous system in membrane function and dysfunction. Febs Letters, 584: 1748-1759.
41. Kabayama K, Sato T, Kitamura F, Uemura S, Kang BW, Igarashi Y, Inokuchi J. (2005) TNFalpha-induced insulin resistance in adipocytes as a membrane microdomain disorder: involvement of ganglioside GM3. Glycobiology, 15: 21-29.
42. Kabayama K, Sato T, Saito K, Loberto N, Prinetti A, Sonnino S, Kinjo M, Igarashi Y, Inokuchi J. (2007) Dissociation of the insulin receptor and caveolin-1 complex by ganglioside GM3 in the state of insulin resistance. Proc Natl Acad Sci U S A, 104: 13678-13683.
43. Lipina C, Hundal HS. (2015) Ganglioside GM3 as a gatekeeper of obesity-associated insulin resistance: Evidence and mechanisms. FEBS Lett, 589: 3221-3227.
44. Chan RB, Oliveira TG, Cortes EP, Honig LS, Duff KE, Small SA, Wenk MR, Shui G, Di Paolo G. (2012) Comparative lipidomic analysis of mouse and human brain with Alzheimer disease. J Biol Chem, 287: 2678-2688.
45. Talbot K, Wang HY, Kazi H, Han LY, Bakshi KP, Stucky A, Fuino RL, Kawaguchi KR, Samoyedny AJ, Wilson RS, Arvanitakis Z, Schneider JA, Wolf BA, Bennett DA, Trojanowski JQ, Arnold SE. (2012) Demonstrated brain insulin resistance in Alzheimer's disease patients is associated with IGF-1 resistance, IRS-1 dysregulation, and cognitive decline. J Clin Invest, 122: 1316-1338.
46. Allen JA, Halverson-Tamboli RA, Rasenick MM. (2007) Lipid raft microdomains and neurotransmitter signalling. Nat Rev Neurosci, 8: 128-140.
47. Xu Y, Sun J, Yang L, Zhao S, Liu X, Su Y, Zhang J, Zhao M. (2022) Gangliosides play important roles in the nervous system by regulating ion concentrations. Neurochem Res, 47: 1791-1798.

48. Hilbush BS, Levine JM. (1992) Modulation of a Ca2+ signaling pathway by GM1 ganglioside in PC12 cells. Journal of Biological Chemistry, 267: 24789-24795.
49. Tanaka Y, Waki H, Kon K, Ando S. (1997) Gangliosides enhance KCl-induced Ca2+ influx and acetylcholine release in brain synaptosomes. Neuroreport, 8: 2203-2207.
50. Watanabe K, Tomono Y. (1984) One-Step Fractionation of Neutral and Acidic Glycosphingolipids by High-Performance Liquid-Chromatography. Analytical Biochemistry, 139: 367-372.
51. Watanabe S, Higashi H, Ogawa H, Takamori K, Iwabuchi K. (2012) Involvement of ganglioside GT1b in glutamate release from neuroblastoma cells. Neuroscience Letters, 517: 140-143.
52. Carlson RO, Masco D Fau - Brooker G, Brooker G Fau - Spiegel S, Spiegel S. Endogenous ganglioside GM1 modulates L-type calcium channel activity in N18 neuroblastoma cells.
53. Wu G, Ledeen RW. Chapter 7 Gangliosides as modulators of neuronal calcium. In: Svennerholm L, Asbury AK, Reisfeld RA, Sandhoff K, Suzuki K, Tettamanti G, Toffano G (szerk.), Progress in Brain Research Vol. 101. Elsevier, 1994: 101-112.
54. Zhao Y, Fan X Fau - Yang F, Yang F Fau - Zhang X, Zhang X. Gangliosides modulate the activity of the plasma membrane Ca(2+)-ATPase from porcine brain synaptosomes.
55. Ando S. (2012) Neuronal dysfunction with aging and its amelioration. Proceedings of the Japan Academy Series B-Physical and Biological Sciences, 88: 266-282.
56. Annunziata I, Sano R, d'Azzo A. (2018) Mitochondria-associated ER membranes (MAMs) and lysosomal storage diseases. Cell Death Dis, 9: 328.
57. Platt FM, d'Azzo A, Davidson BL, Neufeld EF, Tifft CJ. (2018) Lysosomal storage diseases. Nat Rev Dis Primers, 4: 27.
58. Palmano K, Rowan A, Guillermo R, Guan J, McJarrow P. (2015) The Role of Gangliosides in Neurodevelopment. Nutrients, 7: 3891-3913.
59. Schnaar RL. (1994) Isolation of glycosphingolipids. Methods Enzymol, 230: 348-370.

60. Svennerholm L. (1957) Quantitative estimation of sialic acids. II. A colorimetric resorcinol-hydrochloric acid method. Biochim Biophys Acta, 24: 604-611.
61. Wagener R, Kobbe B, Stoffel W. (1996) Quantification of gangliosides by microbore high performance liquid chromatography. J Lipid Res, 37: 1823-1829.
62. Lacomba R, Salcedo J, Alegria A, Jesus Lagarda M, Barbera R, Matencio E. (2010) Determination of sialic acid and gangliosides in biological samples and dairy products: a review. J Pharm Biomed Anal, 51: 346-357.
63. Montealegre C, Verardo V, Luisa Marina M, Caboni MF. (2014) Analysis of glycerophospho- and sphingolipids by CE. Electrophoresis, 35: 779-792.
64. Muthing J. (1996) High-resolution thin-layer chromatography of gangliosides. J Chromatogr A, 720: 3-25.
65. Scandroglio F, Loberto N, Valsecchi M, Chigorno V, Prinetti A, Sonnino S. (2009) Thin layer chromatography of gangliosides. Glycoconj J, 26: 961-973.
66. Yu RK, Ariga T. (2000) Ganglioside analysis by high-performance thin-layer chromatography. Sphingolipid Metabolism and Cell Signaling, Pt B, 312: 115-134.
67. Schnaar RL, Needham LK. (1994) Thin-layer chromatography of glycosphingolipids. Methods Enzymol, 230: 371-389.
68. Kundu SK, Scott DD. (1982) Rapid separation of gangliosides by high-performance liquid chromatography. J Chromatogr, 232: 19-27.
69. Gazzotti G, Sonnino S, Ghidoni R. (1985) Normal-Phase High-Performance Liquid-Chromatographic Separation of Non-Derivatized Ganglioside Mixtures. Journal of Chromatography, 348: 371-378.
70. Ando S, Waki H, Kon K. (1987) New Solvent System for High-Performance Thin-Layer Chromatography and High-Performance Liquid-Chromatography of Gangliosides. Journal of Chromatography, 405: 125-134.
71. Gobburi ALP, Kipruto EW, Inman DM, Anderson DJ. (2021) A new LC-MS/MS technique for separation of gangliosides using a phenyl-hexyl column: Systematic separation according to sialic acid class and ceramide subclass. Journal of Liquid Chromatography & Related Technologies, 44: 114-125.

72. Kirsch S, Muthing J, Peter-Katalinic J, Bindila L. (2009) On-line nano-HPLC/ESI QTOF MS monitoring of alpha2-3 and alpha2-6 sialylation in granulocyte glycosphingolipidome. Biol Chem, 390: 657-672.
73. Meng XY, Yau LF, Huang H, Chan WH, Luo P, Chen L, Tong TT, Mi JN, Yang Z, Jiang ZH, Wang JR. (2019) Improved approach for comprehensive profiling of gangliosides and sulfatides in rat brain tissues by using UHPLC-Q-TOF-MS. Chem Phys Lipids, 225: 104813.
74. Huang Q, Zhou X, Liu D, Xin B, Cechner K, Wang H, Zhou A. (2014) A new liquid chromatography/tandem mass spectrometry method for quantification of gangliosides in human plasma. Anal Biochem, 455: 26-34.
75. Busch CM, Desai AV, Moorthy GS, Fox E, Balis FM. (2018) A validated HPLC-MS/MS method for estimating the concentration of the ganglioside, GD2, in human plasma or serum. J Chromatogr B Analyt Technol Biomed Life Sci, 1102-1103: 60-65.
76. Gu J, Tifft CJ, Soldin SJ. (2008) Simultaneous quantification of GM1 and GM2 gangliosides by isotope dilution tandem mass spectrometry. Clin Biochem, 41: 413-417.
77. Fong B, Norris C, Lowe E, McJarrow P. (2009) Liquid chromatography-high-resolution mass spectrometry for quantitative analysis of gangliosides. Lipids, 44: 867-874.
78. Cantu L, Del Favero E, Brocca P, Corti M. (2014) Multilevel structuring of ganglioside-containing aggregates: From simple micelles to complex biomimetic membranes. Advances in Colloid and Interface Science, 205: 177-186.
79. Ulrich-Bott B, Wiegandt H. (1984) Micellar properties of glycosphingolipids in aqueous media. J Lipid Res, 25: 1233-1245.
80. Yoo YS, Kim YS, Jhon GJ, Park JS. (1993) Separation of Gangliosides Using Cyclodextrin in Capillary Zone Electrophoresis. Journal of Chromatography A, 652: 431-439.
81. Ju DD, Lai CC, Her GR. (1997) Analysis of gangliosides by capillary zone electrophoresis and capillary zone electrophoresis-electrospray mass spectrometry. J Chromatogr A, 779: 195-203.

82. Mechref Y, Ostrander GK, el Rassi Z. (1995) Capillary electrophoresis of carboxylated carbohydrates. I. Selective precolumn derivatization of gangliosides with UV absorbing and fluorescent tags. J Chromatogr A, 695: 83-95.
83. Zamfir A, Vukelic Z, Peter-Katalinic J. (2002) A capillary electrophoresis and off-line capillary electrophoresis/electrospray ionization-quadrupole time of flight-tandem mass spectrometry approach for ganglioside analysis. Electrophoresis, 23: 2894-2903.
84. Hsueh YH, Huang JL, Tseng MC, Her GR. (2010) Sensitivity improvement of CE/ESI/MS analysis of gangliosides using a liquid-junction/low-flow interface. Electrophoresis, 31: 1138-1143.
85. Sarver SA, Keithley RB, Essaka DC, Tanaka H, Yoshimura Y, Palcic MM, Hindsgaul O, Dovichi NJ. (2012) Preparation and electrophoretic separation of Bodipy-Fl-labeled glycosphingolipids. J Chromatogr A, 1229: 268-273.
86. Keithley RB, Rosenthal AS, Essaka DC, Tanaka H, Yoshimura Y, Palcic MM, Hindsgaul O, Dovichi NJ. (2013) Capillary electrophoresis with three-color fluorescence detection for the analysis of glycosphingolipid metabolism. Analyst, 138: 164-170.
87. Wagner Z, Tabi T, Zachar G, Csillag A, Szoko E. (2011) Comparison of quantitative performance of three fluorescence labels in CE/LIF analysis of aspartate and glutamate in brain microdialysate. Electrophoresis, 32: 2816-2822.
88. Carneiro SB, Costa Duarte FI, Heimfarth L, Siqueira Quintans JS, Quintans-Junior LJ, Veiga Junior VFD, Neves de Lima AA. (2019) Cyclodextrin(-)Drug Inclusion Complexes: In Vivo and In Vitro Approaches. Int J Mol Sci, 20.
89. Arima H, Motoyama K, Higashi T. (2017) Potential Use of Cyclodextrins as Drug Carriers and Active Pharmaceutical Ingredients. Chem Pharm Bull (Tokyo), 65: 341-348.
90. Astray G, Gonzalez-Barreiro C, Mejuto JC, Rial-Otero R, Simal-Gándara J. (2009) A review on the use of cyclodextrins in foods. Food Hydrocolloids, 23: 1631-1640.
91. Saokham P, Muankaew C, Jansook P, Loftsson T. (2018) Solubility of Cyclodextrins and Drug/Cyclodextrin Complexes. Molecules, 23.

92. Szejtli J. (1998) Introduction and general overview of cyclodextrin chemistry. Chemical Reviews, 98: 1743-1753.
93. Loftsson T, Brewster ME. (2010) Pharmaceutical applications of cyclodextrins: basic science and product development. J Pharm Pharmacol, 62: 1607-1621.
94. European Medicines Agency (EMA). Cyclodextrins used as excipients Report published in support of the 'Questions and answers on cyclodextrins used as excipients in medicinal products for human use' (EMA/CHMP/495747/2013) Vol. 2022, 2017.
95. Del Valle EMM. (2004) Cyclodextrins and their uses: a review. Process Biochemistry, 39: 1033-1046.
96. Uekaji Y, Jo A, Ohnishi M, Nakata D, Terao K. (2012) A New Generation of Nutra-ceuticals and Cosme-ceuticals Complexing Lipophilic Bioactives with -Cyclodextrin. Procedia Engineering, 36: 540–550.
97. Fenyvesi É, Vikmon M, Szente L. (2016) Cyclodextrins in Food Technology and Human Nutrition: Benefits and Limitations. Critical Reviews in Food Science and Nutrition, 56: 1981-2004.
98. Miyazawa I, Ueda H, Nagase H, Endo T, Kobayashi S, Nagai T. (1995) Physicochemical properties and inclusion complex formation of δ-cyclodextrin. European Journal of Pharmaceutical Sciences, 3: 153-162.
99. Szente L, Fenyvesi E. (2017) Cyclodextrin-Lipid Complexes: Cavity Size Matters. Structural Chemistry, 28: 479-492.
100. Irie T, Otagiri M, Sunada M, Uekama K, Ohtani Y, Yamada Y, Sugiyama Y. (1982) Cyclodextrin-induced hemolysis and shape changes of human erythrocytes in vitro. J Pharmacobiodyn, 5: 741-744.
101. Fenyvesi É, Szemán J, Csabai K, Malanga M, Szente L. (2014) Methyl-Beta-Cyclodextrins: The Role of Number and Types of Substituents in Solubilizing Power. Journal of Pharmaceutical Sciences, 103: 1443-1452.
102. Nishijo J, Moriyama S, Shiota S. (2003) Interactions of Cholesterol with Cyclodextrins in Aqueous Solution. Chemical and Pharmaceutical Bulletin, 51: 1253-1257.

103. Szente L, Szejtli J, Szeman J, Kato L. (1993) Fatty-Acid Cyclodextrin Complexes - Properties and Applications. Journal of Inclusion Phenomena and Molecular Recognition in Chemistry, 16: 339-354.
104. Kilsdonk EP, Yancey PG, Stoudt GW, Bangerter FW, Johnson WJ, Phillips MC, Rothblat GH. (1995) Cellular cholesterol efflux mediated by cyclodextrins. J Biol Chem, 270: 17250-17256.
105. Ottico E, Prinetti A, Prioni S, Giannotta C, Basso L, Chigorno V, Sonnino S. (2003) Dynamics of membrane lipid domains in neuronal cells differentiated in culture. J Lipid Res, 44: 2142-2151.
106. Singhal A, Szente L, Hildreth JEK, Song B. (2018) Hydroxypropyl-beta and -gamma cyclodextrins rescue cholesterol accumulation in Niemann-Pick C1 mutant cell via lysosome-associated membrane protein 1. Cell Death Dis, 9: 1019.
107. Zidovetzki R, Levitan I. (2007) Use of cyclodextrins to manipulate plasma membrane cholesterol content: evidence, misconceptions and control strategies. Biochim Biophys Acta, 1768: 1311-1324.
108. Modi J, Prentice H, Wu J-Y. (2017) Preparation, Stimulation and Other Uses of Adult Rat Brain Synaptosomes. Bio-protocol, 7: e2664.
109. Begley JG, Butterfield DA, Keller JN, Koppal T, Drake J, Mattson MP. (1998) Cryopreservation of rat cortical synaptosomes and analysis of glucose and glutamate transporter activities, and mitochondrial function. Brain Res Brain Res Protoc, 3: 76-82.
110. Daniel JA, Malladi CS, Kettle E, McCluskey A, Robinson PJ. (2012) Analysis of synaptic vesicle endocytosis in synaptosomes by high-content screening. Nat Protoc, 7: 1439-1455.
111. Svennerholm L, Fredman P. (1980) A procedure for the quantitative isolation of brain gangliosides. Biochim Biophys Acta, 617: 97-109.
112. International Conference on Harmonization (ICH). Q2b: Validation of Analytical Procedures: Methodology. . Vol. 2022.
113. Shimamoto K, LeBrun B, Yasuda-Kamatani Y, Sakaitani M, Shigeri Y, Yumoto N, Nakajima T. (1998) DL-threo-beta-benzyloxyaspartate, a potent blocker of excitatory amino acid transporters. Molecular Pharmacology, 53: 195-201.

114. Wagner Z, Tabi T, Jako T, Zachar G, Csillag A, Szoko E. (2012) Chiral separation and determination of excitatory amino acids in brain samples by CE-LIF using dual cyclodextrin system. Analytical and Bioanalytical Chemistry, 404: 2363-2368.
115. Geda O, Tábi T, Lakatos PP, Szökő É. (2022) Differential Ganglioside and Cholesterol Depletion by Various Cyclodextrin Derivatives and Their Effect on Synaptosomal Glutamate Release. International Journal of Molecular Sciences, 23.
116. Otieno AC, Mwongela SM. (2008) Capillary electrophoresis-based methods for the determination of lipids--a review. Anal Chim Acta, 624: 163-174.
117. Roldan-Assad R, Gareil P. (1995) Capillary zone electrophoretic determination of C2·C18 linear saturated free fatty acids with indirect absorbance detection. Journal of Chromatography A, 708: 339-350.
118. Cigić IK, Guček M, Zupančič-Kralj L, Pihlar B. (2003) Separation of isomers of dienoic acids by electromigration techniques. Journal of Separation Science, 26: 1253-1258.
119. Malanga M, Szemán J, Fenyvesi É, Puskás I, Csabai K, Gyémánt G, Fenyvesi F, Szente L. (2016) "Back to the Future": A New Look at Hydroxypropyl Beta-Cyclodextrins. Journal of Pharmaceutical Sciences, 105: 2921-2931.
120. Yong CW, Washington C, Smith W. (2008) Structural Behaviour of 2-Hydroxypropyl-β-Cyclodextrin in Water: Molecular Dynamics Simulation Studies. Pharmaceutical Research, 25: 1092-1099.
121. Ishiguro T, Adachi S, Matsuno R. (1995) Thermogravimetric Analysis of Cyclodextrin-Fatty Acid Complex Formation and Its Use for Predicting Suppressed Autoxidation of Fatty Acids. Bioscience, Biotechnology, and Biochemistry, 59: 51-54.
122. Hoffstetterkuhn S, Paulus A, Gassmann E, Widmer HM. (1991) Influence of Borate Complexation on the Electrophoretic Behavior of Carbohydrates in Capillary Electrophoresis. Analytical Chemistry, 63: 1541-1547.
123. Oefner PJ, Chiesa C. (1994) Capillary electrophoresis of carbohydrates. Glycobiology, 4: 397-412.

124. Stefansson M, Novotny M. (1993) Electrophoretic resolution of monosaccharide enantiomers in borate-oligosaccharide complexation media. Journal of the American Chemical Society, 115: 11573-11580.
125. Geldart SE, Brown PR. (1998) Analysis of nucleotides by capillary electrophoresis. Journal of Chromatography A, 828: 317-336.
126. Tadey T, Purdy WC. (1994) Capillary electrophoretic separation of nucleotide isomers via complexation with cyclodextrin and borate. Journal of Chromatography B: Biomedical Sciences and Applications, 657: 365-372.
127. Nicolaou IN, Kapnissi-Christodoulou CP. (2010) Analysis of polyphenols using capillary zone electrophoresis – Determination of the most effective wine sample pre-treatment method. ELECTROPHORESIS, 31: 3895-3902.
128. Ferrier RJ. Carbohydrate Boronates. In: Tipson RS, Horton D (szerk.), Advances in Carbohydrate Chemistry and Biochemistry Vol. 35. Academic Press, 1978: 31-80.
129. Schmitt-Kopplin P, Hertkorn N, Garrison AW, Freitag D, Kettrup A. (1998) Influence of borate buffers on the electrophoretic behavior of humic substances in capillary zone electrophoresis. Analytical Chemistry, 70: 3798-3808.
130. Pappin B, Kiefel MJ, Houston TA. (2012) Boron-Carbohydrate Interactions. Carbohydrates - Comprehensive Studies on Glycobiology and Glycotechnology, doi:10.5772/50630: 37-54.
131. International Conference on Harmonization (ICH). ICH guideline M10 on bioanalytical method validation and study sample analysis. Vol. 2022, 2022.
132. Thakare R, Chhonker YS, Gautam N, Alamoudi JA, Alnouti Y. (2016) Quantitative analysis of endogenous compounds. Journal of Pharmaceutical and Biomedical Analysis, 128: 426-437.
133. Davidson CD, Fishman YI, Puskas I, Szeman J, Sohajda T, McCauliff LA, Sikora J, Storch J, Vanier MT, Szente L, Walkley SU, Dobrenis K. (2016) Efficacy and ototoxicity of different cyclodextrins in Niemann-Pick C disease. Ann Clin Transl Neurol, 3: 366-380.
134. Nakanishi K, Nadai T, Masada M, Miyajima K. (1992) Effect of cyclodextrins on biological membrane. II. Mechanism of enhancement on the intestinal absorption

of non-absorbable drug by cyclodextrins. Chem Pharm Bull (Tokyo), 40: 1252-1256.

135. Ohtani Y, Irie T, Uekama K, Fukunaga K, Pitha J. (1989) Differential effects of alpha-, beta- and gamma-cyclodextrins on human erythrocytes. Eur J Biochem, 186: 17-22.

136. Maeda Y, Motoyama K, Higashi T, Onodera R, Takeo T, Nakagata N, Kurauchi Y, Katsuki H, Ishitsuka Y, Kondo Y, Irie T, Era T, Arima H. (2019) Lowering effect of dimethyl--cyclodextrin on GM1-ganglioside accumulation in GM1-gangliosidosis model cells and in brain of -galactosidase-knockout mice. Journal of Inclusion Phenomena and Macrocyclic Chemistry, 93: 53-66.

137. Kiss T, Fenyvesi F, Bacskay I, Varadi J, Fenyvesi E, Ivanyi R, Szente L, Tosaki A, Vecsernyes M. (2010) Evaluation of the cytotoxicity of beta-cyclodextrin derivatives: evidence for the role of cholesterol extraction. Eur J Pharm Sci, 40: 376-380.

138. Irie T, Uekama K. (1997) Pharmaceutical applications of cyclodextrins. III. Toxicological issues and safety evaluation. J Pharm Sci, 86: 147-162.

139. Arima H, Motoyama K, Irie T. Recent Findings on Safety Profiles of Cyclodextrins, Cyclodextrin Conjugates, and Polypseudorotaxanes. In: Cyclodextrins in Pharmaceutics, Cosmetics, and Biomedicine, doi:https://doi.org/10.1002/9780470926819.ch5, 2011: 91-122.

140. Monnaert V, Tilloy S, Bricout H, Fenart L, Cecchelli R, Monflier E. (2004) Behavior of alpha-, beta-, and gamma-cyclodextrins and their derivatives on an in vitro model of blood-brain barrier. J Pharmacol Exp Ther, 310: 745-751.

141. Rusznyak A, Malanga M, Fenyvesi E, Szente L, Varadi J, Bacskay I, Vecsernyes M, Vasvari G, Haimhoffer A, Feher P, Ujhelyi Z, Nagy B, Jr., Fejes Z, Fenyvesi F. (2021) Investigation of the Cellular Effects of Beta- Cyclodextrin Derivatives on Caco-2 Intestinal Epithelial Cells. Pharmaceutics, 13.

142. Totterman AM, Schipper NG, Thompson DO, Mannermaa JP. (1997) Intestinal safety of water-soluble beta-cyclodextrins in paediatric oral solutions of spironolactone: effects on human intestinal epithelial Caco-2 cells. J Pharm Pharmacol, 49: 43-48.

143. Roka E, Ujhelyi Z, Deli M, Bocsik A, Fenyvesi E, Szente L, Fenyvesi F, Vecsernyes M, Varadi J, Feher P, Gesztelyi R, Felix C, Perret F, Bacskay IK. (2015) Evaluation of the Cytotoxicity of alpha-Cyclodextrin Derivatives on the Caco-2 Cell Line and Human Erythrocytes. Molecules, 20: 20269-20285.
144. Churchward MA, Coorssen JR. (2009) Cholesterol, regulated exocytosis and the physiological fusion machine. Biochem J, 423: 1-14.
145. Pfrieger FW. (2003) Role of cholesterol in synapse formation and function. Biochim Biophys Acta, 1610: 271-280.
146. Lang T, Bruns D, Wenzel D, Riedel D, Holroyd P, Thiele C, Jahn R. (2001) SNAREs are concentrated in cholesterol-dependent clusters that define docking and fusion sites for exocytosis. Embo Journal, 20: 2202-2213.
147. Salaun C, Gould GW, Chamberlain LH. (2005) Lipid raft association of SNARE proteins regulates exocytosis in PC12 cells. Journal of Biological Chemistry, 280: 19449-19453.
148. Taverna E, Saba E, Rowe J, Francolini M, Clementi F, Rosa P. (2004) Role of lipid microdomains in P/Q-type calcium channel (Ca(v)2.1) clustering and function in presynaptic membranes. Journal of Biological Chemistry, 279: 5127-5134.
149. Xia FZ, Gao XD, Kwan E, Lam PPL, Chan LL, Sy KY, Sheu L, Wheeler MB, Gaisano HY, Tsushima RG. (2004) Disruption of pancreatic beta-cell lipid rafts modifies K(v)2.1 channel gating and insulin exocytosis. Journal of Biological Chemistry, 279: 24685-24691.
150. Xia FZ, Leung YM, Gaisano G, Gao XD, Chen Y, Fox JEM, Bhattacharjee A, Wheeler MB, Gaisano HY, Tsushima RG. (2007) Targeting of voltage-gated K+ and Ca2+ channels and soluble N-ethylmaleimide-sensitive factor attachment protein receptor proteins to cholesterol-rich lipid rafts in pancreatic alpha-cells: Effects on glucagon stimulus-secretion coupling. Endocrinology, 148: 2157-2167.
151. Gil C, Soler-Jover A, Blasi J, Aguilera J. (2005) Synaptic proteins and SNARE complexes are localized in lipid rafts from rat brain synaptosomes. Biochemical and Biophysical Research Communications, 329: 117-124.

152. Tarasenko AS, Sivko RV, Krisanova NV, Himmelreich NH, Borisova TA. (2010) Cholesterol Depletion from the Plasma Membrane Impairs Proton and Glutamate Storage in Synaptic Vesicles of Nerve Terminals. Journal of Molecular Neuroscience, 41: 358-367.

DOI:10.14753/SE.2023.2805

9. Bibliography of the candidate's publications

Publications related to the PhD thesis

1. Geda O, Tábi T, Lakatos PP, Szökő É. (2022) Differential Ganglioside and Cholesterol Depletion by Various Cyclodextrin Derivatives and Their Effect on Synaptosomal Glutamate Release. International Journal of Molecular Sciences, 23.
   IF: 6.208

2. Geda O, Tabi T, Szoko E. (2021) Development and validation of capillary electrophoresis method for quantification of gangliosides in brain synaptosomes. J Pharm Biomed Anal, 205: 114329.
   IF: 3.571

Publications not related to the PhD thesis

1. Lakatos PP, Karádi DÁ, Galambos AR, Essmat N, Király K, Laufer R, Geda O, Zádori ZS, Tábi T, Al-Khrasani M, Szökő É. (2022) The Acute Antiallodynic Effect of Tolperisone in Rat Neuropathic Pain and Evaluation of Its Mechanism of Action. International Journal of Molecular Sciences, 23.
   IF: 6.208

DOI:10.14753/SE.2023.2805

10. Acknowledgements

I would like to express my gratitude all those who contributed to the work presented in this thesis.

I would like to thank my supervisor Prof. Dr. Éva Szökő for giving me the opportunity to undertake this study and for all her guidance throughout my PhD.

I am grateful to Dr. Tamás Tábi, director of the Department of Pharmacodynamics for his help and support during my research work.

I would like to thank Dr. László Tóthfalusi for his advises in statistical analysis and Dr. Péter Pál Lakatos for his contribution in the glutamate measurements.

I am also grateful to my colleagues in the PhD room for the positive environment and encouragement over the years.

I would like to thank my other co-workers at the Department of Pharmacodynamics for their helpful attitude and technical support.

I would like to thank my loved ones for their support during my doctoral studies.

This work was supported by the EFOP-3.6.3-VEKOP-16-2017-00009 grant.